Article:
Jiang, Y., Wang, L., Zhang, B. et al. (6 more authors) (2023) Tunnel lining detection and retrofitting. Automation in Construction, 152. 104881. ISSN 0926-5805

https://doi.org/10.1016/j.autcon.2023.104881

Tunnel lining detection and retrofitting

Yandan Jiang[1], Lai Wang[1], Bo Zhang[4], Xiaowei Dai[2], Jun Ye[2,3,6], Bochao Sun[2], Nianwu Liu[4], Zhen Wang[5], Yang Zhao[2,3]

1. State Key Laboratory of Industrial Control Technology, College of Control Science and Engineering, Zhejiang University, Hangzhou, China, 310027

2. College of Civil Engineering and Architecture, Zhejiang University, Hangzhou, China, 310058

3. Center for Balance Architecture, Zhejiang University, Hangzhou, China, 310058

4. School of Civil Engineering and Architecture, Zhejiang Sci-Tech University, Hangzhou, China, 310018

5. Department of Civil Engineering, Zhejiang University City College, Hangzhou, China, 310015

6. Centre for Intelligent Infrastructure, University of Strathclyde, Glasgow, UK, G1 1XJ

ABSTRACT: The underground tunnel structure is important and common in transport infrastructures. With the increasing service time, it is crucial to detect the deteriorations in the ageing tunnel linings and make informed retrofitting decisions to ensure their structural safety and extend their service life cycle. This emphasizes the importance of understanding the framework of tunnel lining detection, evaluation, and retrofitting. However, there is no up-to-date review available that covers the entire workflow of tunnel lining detection and retrofitting. This paper provides a comprehensive review of non-destructive testing (NDT) methods, health evaluation methods, and retrofitting methods for tunnel linings. The achievements, challenges, and development trends of these methods are illustrated. Specifically, NDT methods for three representative tunnel lining defects, including cracks, leakage, and voids, are introduced and analyzed to show the corresponding advantages and disadvantages. Based on the data obtained by the defect detection methods, the procedures for lining health status evaluation are also summarized to provide a systematic and quantitative evaluation of tunnel linings. Finally, the retrofitting methods and techniques that are suitable for lining structures are reviewed. This paper provides an insight into the development of structural health monitoring (SHM) and the maintenance of tunnel linings, offering a systematic guide for understanding the framework of tunnel lining detection and retrofitting.

KEY WORDS: Tunnel lining; Defects; Non-destructive testing; Evaluation; Reinforcement; Retrofitting

1. Introduction

Transportation infrastructure has been developed rapidly during the past decades due to the issues of increased population and traffic congestion [1–3]. Among them, the tunnel structures have become more and more important due to their high construction efficiency and the limited space in urban areas [4]. With the popularity of tunnel structures, the travel efficiency has been significantly improved and transportation costs have been dramatically reduced. In 2019, there were 1615 tunnel projects globally under construction, and 2615 tunnels under planning [5]. China has built over 30,000 km of traffic tunnels and is constructing or planning more than 40,000 km to meet city expansion demands [6]. Japan has built 5,098 km of traffic tunnels, some are over 50 years old but are still in service [7]. However, a significant problem is that many tunnels entered the "maintenance and repair" life cycle [8]. After long-term service, some tunnels exhibit significant health issues, such as lining cracking, water leakage, and voids behind the linings [8,9]. Since the linings are important structural components of the tunnel, accurate detection, periodic monitoring of their status and timely maintenance are crucial to ensure safe operations.

As the service time increases, the structural health of tunnel linings gradually deteriorates due to ageing, long-term loading, and environmental factors [10]. Inadequate maintenance accelerates this process, therefore tunnel structure failures occur frequently [11]. In 2012, over 300 concrete ceiling panels collapsed in the Sasago Tunnel in Japan, resulting in significant damage to the tunnel structure [12]. The collapse of approximately 10 m^2 of tunnel lining in 2020 caused damage to a vehicle and resulted in life loss [13]. These accidents from the failure of tunnel linings caused a threat to the safety of the traffic and human lives. To mitigate these risks, it is increasingly important to use structural health monitoring (SHM) data and appropriate damage assessment methods to detect and evaluate the defects in the linings and adopt effective means of maintenance and reinforcement on demand to reduce the risk of lining failures [14–16].

Qualitative and quantitative detection of tunnel lining defects is essential for subsequent evaluation and reinforcement. With the rapid development of non-destructive testing (NDT) techniques, a wide range of tunnel lining inspection methods has been developed, including vision-based methods, acoustic techniques, infrared thermography, radar, electrical techniques [17], etc. In recent years, these traditional NDT methods in combination with artificial intelligence and robotics

have emerged as a new research focus [18–20]. Previous literature reviews help us to understand the development of the methodology in a specific structure, defect, or technique, including infrastructure inspections [16,19,21,22], targeting at a single type of defect like crack [18], or a single detection method, such as computer vision [10,16,18,19], ground-penetrating radar (GPR) [22], acoustic techniques [23] and robotic techniques [24]. These review papers are summarized and compared in **Appendix 1**. However, there are no specific overviews of NDT techniques for detecting the various defects in tunnels. With the rapid development of detection technology and the increasing demand for tunnel inspection, it is beneficial to summarize the latest detection methods to provide a comprehensive review of tunnel inspection.

Based on the data obtained from tunnel inspection, the health issues of the tunnel can be assessed. The evaluation methods can be qualitative or quantitative according to the characteristics of the defects [25]. Typically, the overall condition evaluation of the tunnel is carried out by Expert Methods [26]. With the in-depth exploration of the ageing mechanism of architectural structures and the development of the detection methodology, new evaluation techniques have been proposed by researchers [24,27]. As more and more evaluation methods are available [28–30], the evaluation framework for the tunnels is gradually forming. It includes three main steps: presentation of evaluation criteria, selection of evaluation parameters, and derivation of evaluation results. From previous studies, the boundary between detection and evaluation is not always clear [24,27]. There is a lack of reviews sorting the effective methods for structural health assessments of tunnel linings (summarized as **Appendix 2**). Therefore, a review of the structural assessment methods and their classifications according to the characteristics of various defect detection methods targeting at tunnel linings is needed.

With the results of tunnel inspection and health assessment, retrofitting decisions can be made. Once the evaluation shows that the conditions of reinforcement are met, timely retrofitting of tunnel linings is crucial to extend the lifespan of tunnels [31]. The tunnel retrofitting has been one of the main research focuses over the last few decades [31–40], as shown in **Appendix 3**. Previous studies provided brief summaries of tunnel strengthening methods related to the actual tunnel projects. Therefore, the various retrofitting methods, including their rationales, advantages, disadvantages, and future development, have not been specifically reviewed yet. A systematic organization and

analysis of these details should be conducted.

In conclusion, there is no review available that systematically covers the entire workflow of tunnel lining detection, assessment, and retrofitting. As shield tunnels become more and more widely used, there is a need for an up-to-date review and summary that can address these issues. This paper is to provide a comprehensive literature review covering the entire framework of tunnel lining detection and retrofitting, including the detection techniques for different defects, the scientific evaluation methods of structural health, and the effective retrofitting methods. The state of the art of different techniques/methods targeting at tunnel lining detection and retrofitting is presented. The advantages, disadvantages, correlation, and contradiction of different methods are also compared and discussed. This review can help researchers to have a rapid systematic understanding of the various aspects of tunnel lining detection and retrofitting, and have an idea of the challenges that remain to be overcome.

The review will be structured as follows: **Section 2** reviews the classical detection methods of tunnel lining defects and their applications. **Section 3** summarizes the existing evaluation methods of tunnel lining conditions. **Section 4** presents the available tunnel retrofitting methods and **Section 5** concludes the state-of-the-art review, followed by some discussions, challenges and the research to be undertaken in the future.

2. Tunnel lining defects and detection methods

Understanding the different categories of defects in tunnels is critical for exploring effective detection methods. Although classifications of tunnel defects in existing studies differ slightly, they can be divided into several types. The most commonly observed defects of tunnel linings include cracks, leakage, and voids [41–45]. **Fig. 1** demonstrates the three types of defects. Although there are some relationships between different defects [13], cracks are the most commonly observed form of tunnel lining damage and attract significant attention from researchers [19]. The voids behind the lining are the main cause of cracks while the leakage often occurs at cracks [13]. These defects can be identified and detected by different techniques according to different physical mechanisms. However, the inspection and assessment of these defects are still challenging due to the limited access to the internal space of the tunnel lining structures.

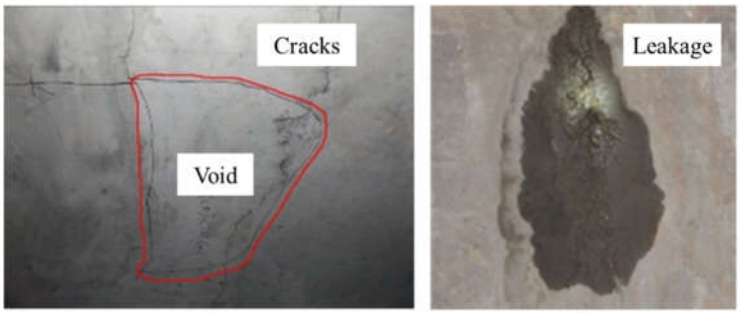

Fig. 1. Typical tunnel lining defects: (a) cracks and void [13]**; (b) leakage** [46]**.**

2.1 Cracks

Cracks possess a morphological feature with elongated and high-contrast edges and lead to changes in the lining structure. As such, they can be detected through various physical methods, including visual inspection, radar, and acoustic techniques [17].

Conventional visual inspection of tunnel lining cracks relies heavily on manual labor [19]. However, the operator is exposed to the dangerous tunnel environment, including large isolated areas, low visibility, dust, humidity or even toxic gases [24]. Additionally, the subjectivity and inefficiency of this approach in obtaining data for structural evaluation are still issues to be addressed in the future.

To achieve more efficient, accurate, and standardized crack inspections, photogrammetric and vision-based methods have been proposed [19]. And currently, vision-based methods are generally considered to be the most popular NDT methods in tunnel inspections. **Fig. 2** shows a typical structure of an image acquisition system for tunnel lining, including a group of linear array cameras, a group of laser sources, a control and image acquisition unit, and an industrial personal computer (IPC). These components are usually mounted on a track inspection train for mobile inspections [47].

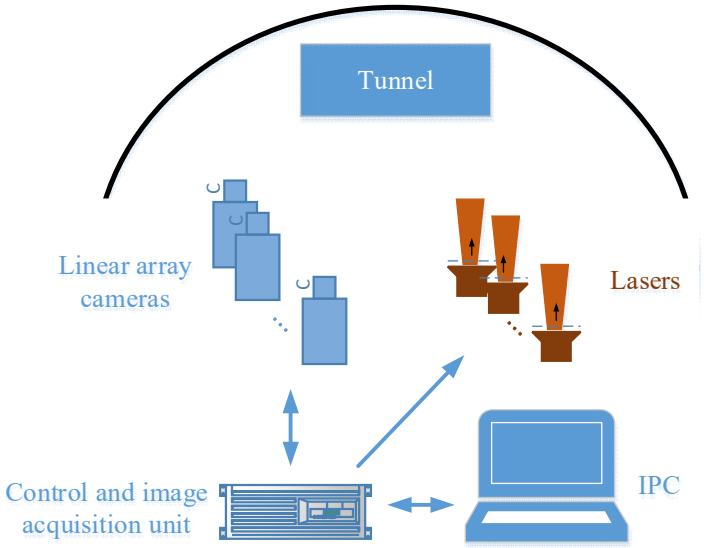

Fig. 2. Typical structure of the image acquisition system.

Benefiting from image processing technology, vision-based methods have experienced rapid development over the past decades. Conventional image processing methods for crack detection include threshold techniques, morphological operators, texture analysis, pattern recognition, etc. [10]. **Fig. 3** shows a common flowchart of digital image processing for crack detection, including image enhancement, image processing (segmentation and feature extraction), and crack analysis. The results of image processing are used for subsequent qualitative or quantitative analysis. Lei et al. [48] proposed a tunnel lining crack recognition system that employs a series of image processing methods. An effective segmenting method, combining adaptive partitioning, edge detection, and threshold technique, was presented, and the size of cracks was calibrated for precise quantification. Research results demonstrated a deviation of less than 20% in the measurement of crack sizes between the proposed system and manually measured field tests. Gong et al. [47] used multiple line scan cameras to collect the full images of tunnel lining surfaces and proposed an automatic crack detection method. Image threshold segmentation and edge threshold were used to obtain the morphological and gradient features of the crack, and cracks were extracted using the seed-filling algorithm. Additionally, the proposed method can effectively eliminate interference, such as pipeline edges and strip marks, through multistage fusion filtering. Wang et al. [49] proposed a method that combined the improved multiscale Retinex (MSR) algorithm for filtering and the eight-direction Sobel operator for edge extraction. A recognition rate of 97.5% was obtained and the

processing efficiency of the algorithm was relatively high. Considering the impact of image quality, such as low contrast and uneven illumination, on the effectiveness of crack detection, Yu et al. [50] used infrared images instead of visible light images. The authors computed the conditional texture anisotropy of each pixel and obtained the optimum threshold through iteration to extract the cracks. The proposed method was applied to 50 crack images with different background and illumination conditions, resulting in better recognition effectiveness than histogram estimation and Otsu algorithm. The above conventional image processing methods have made significant progress in improving the crack detection performance of vision-based methods, including recognition rate, detection efficiency and robustness. However, they share a common limitation, which is the selection of the optimum threshold for image segmentation. This step can be troublesome and has a significant impact on the effectiveness of the detection.

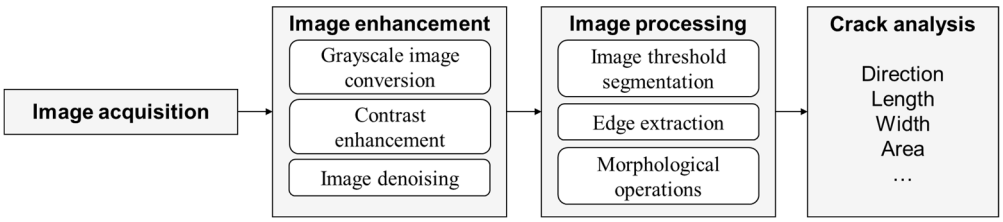

Fig. 3. Flowchart of conventional image processing.

With the development of machine learning (ML) and deep learning (DL), the quality of crack detection has been significantly improved in recent years [18]. Compared to conventional image processing methods, the feature extraction of ML/DL methods is automatically performed during the training process, without the need to determine the optimum threshold. Hsieh and Tsai [18] divided DL crack detection into three task categories, classification, object detection, and segmentation, as shown in **Fig. 4**. The authors reviewed 68 ML-based crack detection methods and summarized their trends. They observed that the patch-level classification was more popular before 2016, but segmentation methods have been rapidly developed after that, providing higher-resolution data and more precise crack detections. They also found that deeper backbone networks in fully convolutional network (FCN) models and skip connections in u-shaped network (U-Net) models had satisfactory performance after evaluating eight crack segmentation models. Xue and Li [51] proposed a fully convolutional network (FCN) for classification and a region proposal network

(RPN) and position-sensitive region of interest (RoI) pooling for defects detection. After comparing with AlexNet (ISVRC2012), GoogLeNet (ISVRC2014), and VGG16 (ISVRC2014), their model achieved a best-set accuracy of over 95% at a test time of 48 ms. It also outperformed the conventional methods and region-based faster CNN (Faster R-CNN) in terms of detection rate, detection accuracy, and detection efficiency. Ren et al. [52] proposed an end-to-end pixel-wise crack segmentation algorithm based on an improved deep FCN called CrackSegNet, the architecture of which is shown in **Fig. 5**. The network combined the advantages of FCN, U-Net, and Pyramid Scene Parsing Network (PSPNet) and was improved based on the characteristics of the crack dataset. Compared to the conventional methods and the FCN, CrackSegNet had a higher detection accuracy. Xu and Yang [53] developed a method combining geometric modeling and a crack detection algorithm. The B-spline surface approximation algorithm was used to construct a three-dimensional tunnel model, and a mask region-based convolutional neural network (Mask R-CNN) was deployed for crack segmentation. Their method provided a significant solution for intelligent tunnel monitoring. Zhao et al. [54] presented a method for crack segmentation and quantification, where they utilized a path aggregation network (PANet) model to detect cracks and an A* algorithm in the semantic branch to measure the size of the cracks. In their work, the proposed method had a lower error rate than the medial axis algorithm in crack quantification. Li et al. [55] designed a data collection system for image acquisition and proposed a multi-layer feature fusion network based on the Faster R-CNN for defect detection. The enhanced network had a good performance in practical field tests, but it did not run in a real-time image processing system.

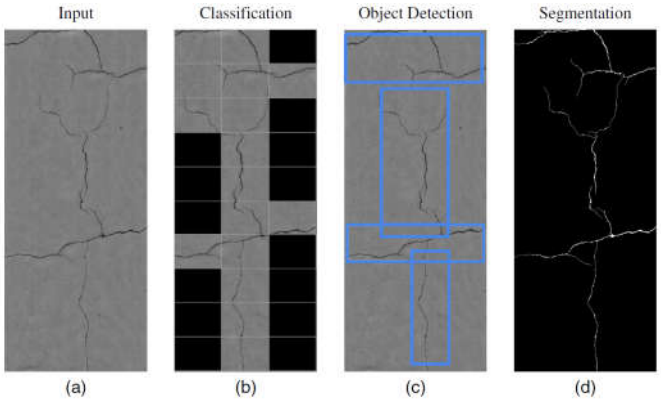

Fig. 4. (a) Input image of cracks; (b) classification; (c) object detection; and (d) segmentation [18].

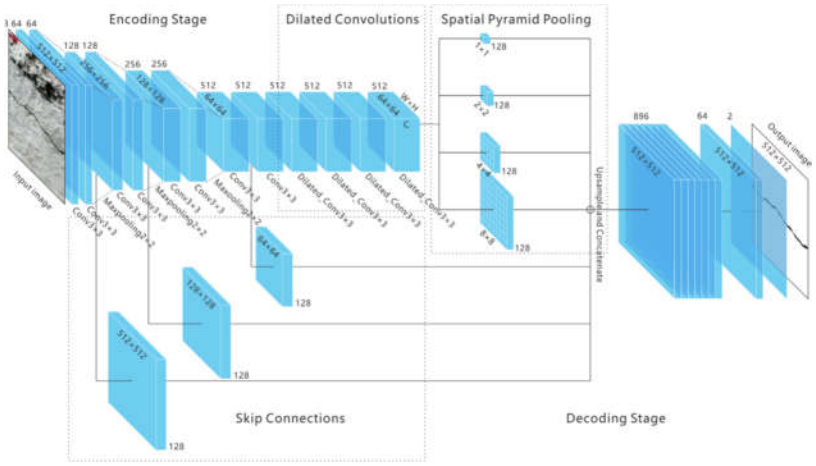

Fig. 5. Network architecture of CrackSegNet [52]**.**

In previous reviews, Attard et al. [10] explained the image processing techniques for detecting cracks and other defects in detail. Koch et al. [19] presented a summary of defect detection based on computer vision and condition assessment for several types of civil infrastructure, and part of the content described the visual inspection approaches of concrete tunnel cracks. Both of them provided useful insights into the vision-based detection methods of tunnel lining defects. Although vision-based methods are currently the dominant means of tunnel lining inspection, their limitation is clear. Vision-based methods rely on what is visually observed, which means only surface defects and crack size on the surface can be detected and measured, the internal defects and the crack depth information cannot be obtained. Therefore, other detection techniques are needed to provide more comprehensive essential data.

Another technique used for crack detection is GPR. GPR has been widely used in geophysics and related disciplines [20,56]. It uses electromagnetic fields to detect the lossy dielectric materials and obtain the subsurface status by analyzing the characteristics of the reflected echoes, such as travel time, amplitude, phase velocity, and attenuation with frequency [56]. GPR has been used in the detection of tunnel lining defects, including cracks. **Fig. 6 (a)** illustrates the construction of the GPR device, which consists of antennas for transmitting and receiving electromagnetic waves, a radar control unit with the function of processing GPR data, and other auxiliary structures [57]. **Fig. 6 (b)** shows the basic principle of GPR for crack detection. When the electromagnetic wave encounters an object with physical properties different from the surrounding medium, then it is scattered from the target and detected by the receiving antenna. A 2D image can be constructed after

post-processing. Xiang et al. [58] used GPR in the Damaoshan highway tunnel and obtained results including rebar position, second lining thickness, and probable defects behind the lining. Several probable internal cracks were revealed through the anomalous areas in the GPR data profiles. **Fig. 7** showed the damage radargrams obtained by GPR, where B and C indicated the features of cracks or fissures. Feng et al. [59] proposed a hybrid algorithm that combines finite-difference time-domain (FDTD) and finite-element time-domain methods for GPR simulation and built numerical models of various defects in the tunnel lining. It is worth noting that GPR is mainly applied to the inspection of internal conditions, with only a few studies exploring its application in surface crack detection, crack depth measurement [60], and micro-crack detection [61]. Ling et al. [61] explored the feasibility of distinguishing the weak reflected signal corresponding to the micro-cracks among the complicated signal by using the orthogonal matching pursuit and the Hilbert transform (OMHT) method. This method could significantly enhance the weak signal and improve the resolution of the GPR image. In terms of detection accuracy and resolution, the GPR is heavily dependent on data interpretation. Besides, the selection of antenna frequency and the design of the antenna are critical to the detection performance as well. Although the work mentioned above provides some useful references, these difficulties remain as an important focus of future research.

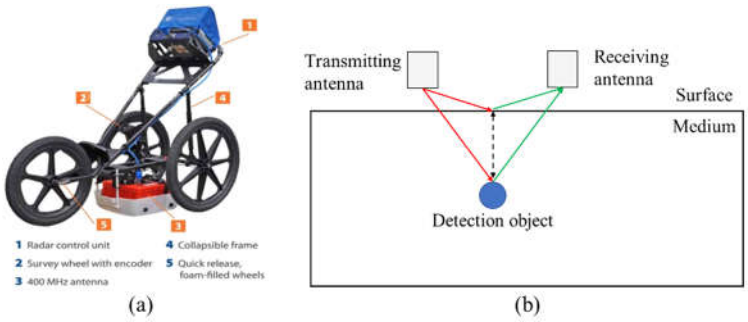

Fig. 6. (a) The GPR radar GSSI SIR 3000 and (b) principle of GPR [57]**.**

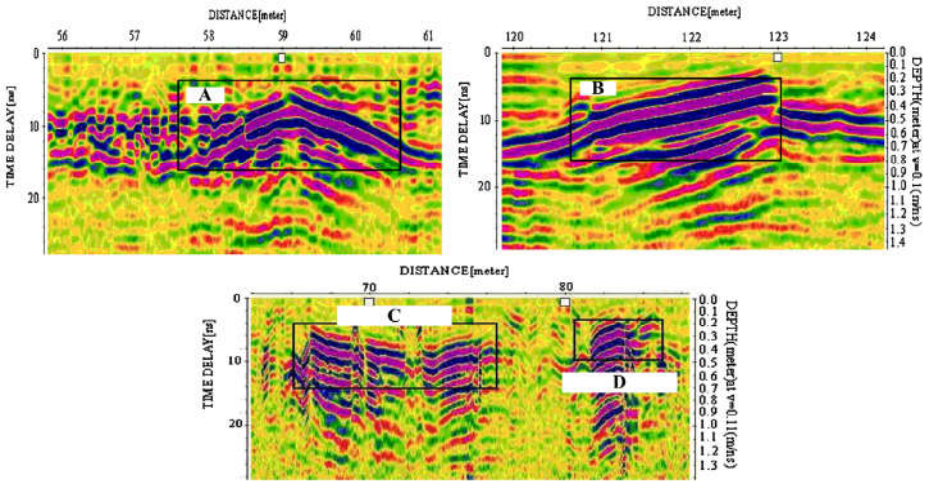

Fig. 7. Damage radargram of left haunch (A and B) and vault profile (C and D) [58]**.**

Sonic and ultrasonic techniques are effective NDT methods for unilaterally accessible concrete structures such as tunnel linings or thick concrete walls [23,62–69]. There is a category of techniques, including the impact-echo technique, Time-Of-Flight Diffraction (TOFD), impulse response technique, ultrasonic tomography technique, and others. In crack detection, the transmission and diffraction of acoustic waves inside the medium can provide useful information for measuring crack size. The TOFD technique can successfully detect the diffraction of acoustic waves at the edges or tips of defects to obtain the position and size of cracks [62,63]. **Fig. 8** shows the measurement principle of TOFD. When an acoustic signal is emitted by the transmitter, the tips of the crack will diffract the ultrasound beam. This diffracted beam can then be detected by the receiver and the arrival time can be accurately measured. The depth and size of the crack can be calculated according to **Eq. (1)** [62].

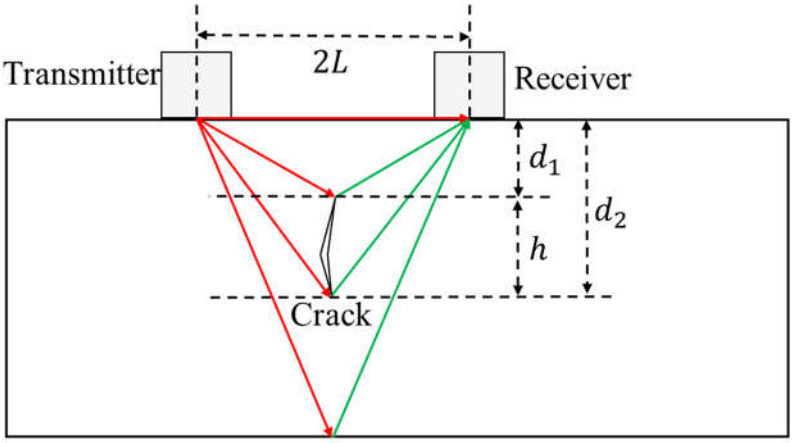

Fig. 8. Principle of TOFD.

$$d = \sqrt{\left(\frac{c \cdot \Delta t}{2}\right)^2 - L^2}$$

$$h = d_2 - d_1 \quad (1)$$

where d is the depth of the upper or lower tip of the crack, c is the velocity of sound, Δt is the travel time of the ultrasound beam, L is half of the distance between the transmitter and receiver, and h is the length of the crack. Habibpour-Ledari and Honarvar [64] extended the TOFD technique from 2D space to 3D space and developed an active algorithm based on the time-of-flight of the echoes. The proposed algorithm was tested in defect location experiments and achieved a precision of 6.7%, which was lower than the passive algorithm. However, it had fewer limitations on the number of receivers than the passive algorithm, making it a viable option for practical applications. Moreover, the reflection, transmission, and scattering of Rayleigh surface wave transmission (SWT) across a surface-breaking crack have also been studied [65,66]. **Fig. 9** shows the corresponding measurement principle of the SWT test [67]. In the SWT method, two sensors are located on the two sides of the crack, respectively. The depth of the crack can be estimated from the transmission coefficient, which is defined as the spectral amplitude ratio between the transmitted surface waves R_{tr} and the incident surface waves R_i in the frequency domain [67]. Angel and Achenbach [65] obtained the curve for the transmission coefficient versus the frequency under the constraint of fixed incidence angle through theoretical derivation. Yew et al. [66] also estimated the relationship between the crack depth and the amplitude of the transmitted surface wave through experimental study. This early work provided an important theoretical basis for subsequent sensor development and signal processing. Since the traditional acoustic techniques for crack inspection require direct contact between the devices and the concrete surface, which is time-consuming and requires adequate coupling, several non-contact air-coupled SWT-based sensors have been developed [68,69]. This type of sensor can also achieve rapid measurement of crack depth. Kee and Zhu [68] used numerical simulations, based on the finite element method (FEM), to investigate the near-scattering of surface waves caused by a surface breaking crack in concrete and compared it with the surface wave transmission measured in the far field. It is showed that surface wave transmission measurements in the far field could effectively avoid near-field effects. The

measurement results also showed a high degree of consistency with the analytical results. Moreover, both of them verified the curve for the normalized transmission coefficient versus the normalized crack depth proposed by Angel and Achenbach [65]. In addition, a simplified algorithm using only the transmission value at the center frequency was proposed and experimentally verified. A more detailed description of the study on crack detection in concrete structures using SWT-based sensors can be found in the work of Kee et al. [67]. In et al. [69] investigated a fully non-contact ultrasonic sensor using air-coupled transducers and reconstructed the relationship between the transmission coefficient and the normalized notch depth, as shown in **Fig. 10**. In the measurement, the elastic waves were generated by the sensors, and mechanical contact was no longer required. These sensors were of higher repeatability, and the experimental results showed satisfactory consistency agreement with the numerical simulations. The sensors were expected to be used for mobile continuous monitoring after improving penetration depth and stability. However, in these tests, the sensors were applied to a specimen with a shallow notch instead of a real crack with an irregular shape and depth. To achieve non-contact measurements, special ultrasonic sensors capable of generating high-energy excitation signals are often required. Although these works have not been specifically applied to the detection of tunnel lining cracks, they provide a beneficial reference for field inspection, especially when used for the size measurement of cracks. For complex NDT tasks, a combination of these techniques could be a good choice. Non-destructive acoustic techniques for the inspection of concrete structures and their detailed applications and limitations can be found in the work by Schabowicz [23]. The author introduced a method that combined ultrasonic tomography and the impact-echo technique to determine the position of cracks with a detection accuracy of 5-10 mm.

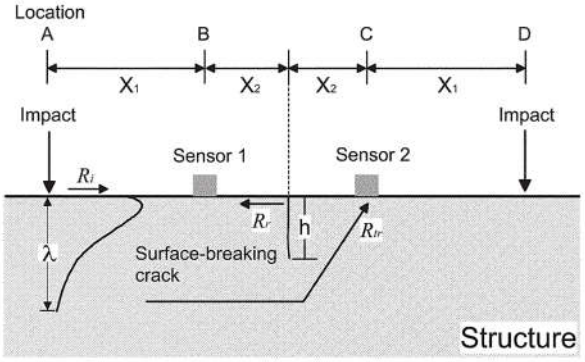

Fig. 9. Principle of SWT test [67]**.**

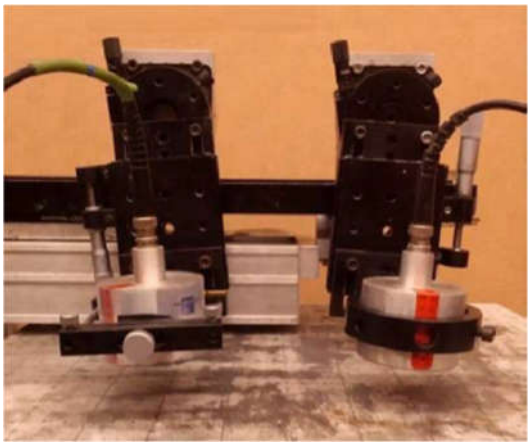

Fig. 10. The non-contact, air-coupled ultrasonic sensors [69]**.**

A more intuitive way to detect a crack is to visualize the crack in terms of images. Tomography is one of the best methods to visualize defects [70,71]. It uses the information obtained from the projections calculated by the measurements of a specifically designed sensor array to perform inversion calculations to reconstruct the distribution of the medium inside the object. In addition to the previously mentioned ultrasonic tomography, electrical tomography is another tomographic technique that can be potentially applied to the crack detection of tunnel linings. It can present the electrical impedance distribution inside the concrete structure through image reconstruction algorithms. Electrical resistance tomography (ERT), electrical capacitance tomography (ECT), and electromagnetic tomography (EMT) are three common modalities in the electrical tomography family. Karhunen et al. [70] used ERT to visualize the position and size of the crack in the cylindrical concrete specimen. To investigate its performance in realistic single-side inspection scenarios, they tested the feasibility of the above ERT system on the planar surface of concrete [71]. The photographs of the specimen beam and the reconstruction results are shown in **Fig. 11**. The crack in the beam after the three-point bending test extends to the middle of the specimen and can be seen in **Fig. 11 (b)**. Electrical tomography has many advantages such as low cost, high speed, and good real-time performance. However, electrical tomography has not yet been applied to the field detection of tunnel lining defects yet because of its low resolution.

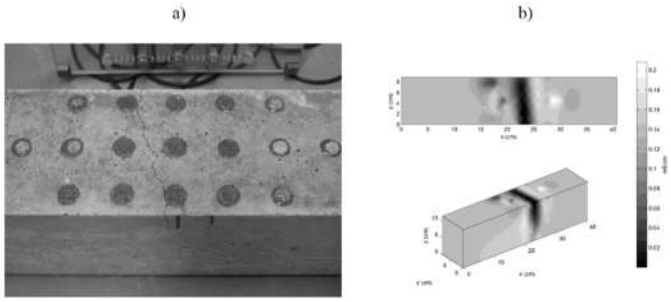

Fig. 11. (a) Photograph of specimen; (b) ERT results [71]**.**

Different inspection methods have their advantages, disadvantages, and scope of applications, which means relying solely on one technique typically leads to limited detection performance. To obtain more information and improve detection accuracy, researchers have made progress in multi-sensor fusion and the integration of detection methods [20,25,47,48,72]. Mobile vehicles and robots are the carriers of integrated detection methods such as visible light or infrared cameras, radar, laser scanners, and acoustic sensors to achieve automatic tunnel inspection. The image acquisition system on the vehicle consists of cameras and lighting equipment [47,48], which can scan the lining surface at high speed to reduce the impact on tunnel traffic. Jiang et al. [25] proposed a tunnel lining inspection system, which integrated the lining scanning system including the near-infrared ray illumination and line sensor cameras, lining surface image creation software, and crack extraction software (**Fig. 12**). The system was able to photograph the lining at a maximum speed of 100 km/h and automatically detect and assess the cracks. Mobile inspection vehicles have a strong carrying capacity and integrate several pieces of equipment, such as line scan cameras, laser scanners, and radars, so they can detect different tunnel defects and have been widely used in field inspection [72]. With the development of mobile robot technology, completely unmanned tunnel inspection gradually becomes a reality. The ROBO-SPECT European project [20] achieved an automated tunnel inspection using the robotic system (**Fig. 13**) which included the vision system to detect tunnel lining defects, the laser profilers to inspect tunnel structure deformation, and the ultrasonic sensors to measure the size (width and depth) of the cracks after detecting them. The measured results can be used in subsequent damage assessments. In terms of the advantages of robots over detection vehicles, robots are more flexible and have stronger information fusion and communication capabilities.

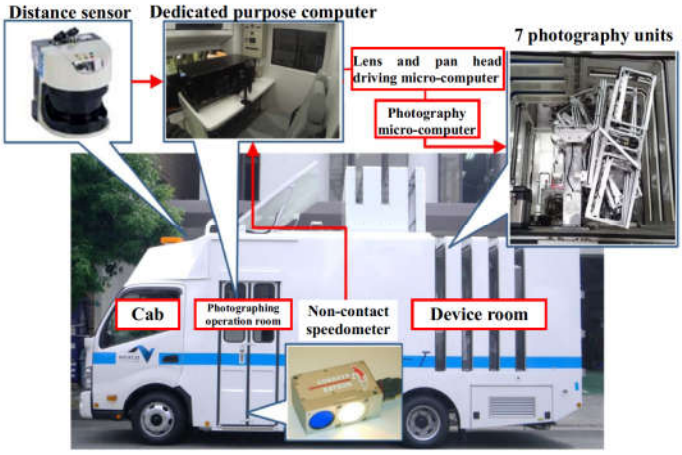

Fig. 12. The tunnel lining surface photography vehicle components [25].

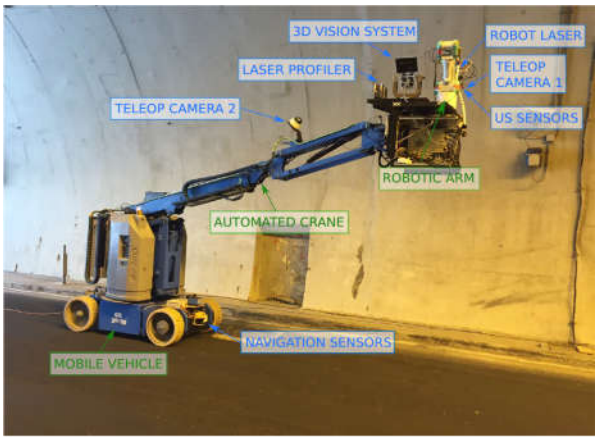

Fig. 13. The ROBO-SPECT robotic system components [20].

In general, vision-based techniques are the most commonly used NDT methods for the detection of tunnel lining surface cracks because of their advantages in data acquisition, efficiency, and accuracy. As the direction, location, type, and size of cracks are important parameters of interest to researchers and engineers, other NDT methods are necessary to provide supplemental source information, such as subsurface cracks and other quantitative crack information.

2.2 Leakage

Water leakage is a frequent problem that occurs at lining cracks and lining joints, mainly in the sidewalls, and is greatly influenced by seasonal rainfall [13]. It can damage tunnel lining and affect the function of the structural components. Similar to crack detection, image processing techniques

can also detect leakage instead of relying on manual visual inspections. The leakage area is typically darker than the background area, with an obvious edge and vertical directionality due to gravity [10]. These visual features make edge detection and threshold segmentation convenient. Huang et al. [73] developed moving tunnel inspection equipment that captured images of the tunnel lining with CCD cameras. The leakage was then recognized by image edge detection and the Otsu algorithm [74], which was used to calculate the optimal threshold for segmenting the leakage area. However, conventional image processing methods are sometimes not a good choice in detecting leakage because of the interference from surface stains or attachments in the tunnel.

Deep learning-based methods are expected to improve the accuracy of detecting leakage and have shown satisfactory performance in recent years [46,51,55,75,76]. In addition to crack detection, the methods proposed by Xue and Li [51] and Li et al. [55] also showed accurate and efficient performance in detecting leakage. In the follow-up work by Huang et al. [75], upgraded image acquisition equipment was developed to acquire tunnel lining images, and a two-stream algorithm using FCN models was applied to segment overlapped regions of crack and leakage. The proposed algorithm achieved error rates of 1.1%, 2.1%, and 1.5%, respectively, in the leakage recognition of several defect images, including leakage-only images, two-defect-nonoverlapping images, and two-defect-overlapping images. Segmenting overlapped defects was highly necessary because leakage always occurred at cracks, and this work made a beneficial attempt. Xue et al. [76] also improved the performance of their deep learning-based model for leakage segmentation through data augmentation, transfer learning, and a cascade strategy. They obtained the leakage area by calibrating the relationship between the leakage area pixels and the true leakage areas, followed by estimating the safety status of the tunnel lining. Zhao et al. [46] proposed a method that combined the ResNet-101 and Mask R-CNN to classify and segment defect images. In the integrated progress, the combination of classification and segmentation methods achieved an accuracy of 89.3%. Deep learning-based methods enabled machines to achieve automatic and robust defect detection after acquiring image sets containing a large number of lining defect images. They showed better performance than conventional image processing methods for single or mixed tunnel lining defects. The features were extracted automatically for follow-up tasks, including classification, object detection, and segmentation. However, deep learning-based methods also have limitations and

problems, such as being regarded as a black-box technique that is difficult to explain physically and relies heavily on large datasets.

The above methods are based on visible light images, whose quality is inevitably affected by the practical complex environment and the confusing background [10]. An effective alternative to the visible light image is the thermal infrared image, which will not be affected by environmental light [50]. Any object with a temperature higher than 0 K will emit thermal radiation. According to the Stefan Boltzmann Law (**Eq. (2)**), the radiation energy is related to the temperature of the object:

$$Q = \varepsilon \sigma T^4 \tag{2}$$

where Q is the radiation in W/m^2, ε is the emissivity of the object with a range of 0–1, σ is the Stefan Boltzmann constant ($5.67 \times 10^{-8} W m^{-2} K^{-4}$), and T is the surface temperature in K [77]. The temperature distribution characteristics of different types of water leakage can be seen in **Fig. 14**. Due to the different types of water leakage, such as spot-leakage type and slot-leakage type, their temperature distribution characteristics are also significantly different. However, overall, they exhibit a temperature distribution where the temperature at the leakage source/centre is lower, which is due to the higher ambient temperature. It is useful for identifying leakage by detecting the difference between the leakage area and the background lining in the infrared radiation temperature field. Infrared thermography includes both passive and active techniques. The former refers to the detection of natural temperature differences, while the latter refers to the detection of temperature differences after active heating, mainly for detecting deep subsurface defects. In practice, a thermal infrared camera can accurately identify a very small temperature difference (approximately 0.05 °C) within the temperature range of -20℃~+150℃ [78]. Most researches on the application of infrared thermography in tunnel leakage detection focused on the passive infrared thermography technique. Conventional image processing techniques, such as edge detection and threshold segmentation, can also be applied to thermal infrared images. Yu et al. [78] proposed a method based on laser scanning and infrared thermal imaging to detect water leakage in tunnels. After the suspected leakage area was detected from the laser intensity data, thermal infrared images were obtained to verify the leakage, distinguish the types of leakage, and determine the leakage location and direction. Lu et al. [79] introduced an automatic inspection system for cable tunnel leakage detection based on infrared thermography. **Fig. 15** shows the inspection system, including a passive infrared thermography

device, an ultrasonic sensor, a visible camera, and a photoelectric encoder. The control PC was connected to the inspection vehicle via WI-FI to control its movement and image acquisition, which was then processed and analyzed in real time or offline. As shown in **Fig. 16**, the processing of the thermal infrared image containing the leakage area went through several steps, namely gray processing, filtering, binarization, and threshold segmentation. Additionally, the system could accurately calculate the leakage point area and subsequently provide an objective assessment report. The inspection vehicle, however, was not automatic and instead relied on the connection to the control computer, which could lead to limitations in certain operating conditions. The passive infrared thermography method has the advantages of fast data acquisition and high accuracy, which is sufficient to detect surface leakage on the tunnel lining. However, infrared thermography may be affected by complex noise, such as thermal reflection from other heat sources [77]. The low signal-to-noise ratio (SNR) caused by infrared cameras and environmental factors requires more accurate and reliable methods for tunnel leakage detection.

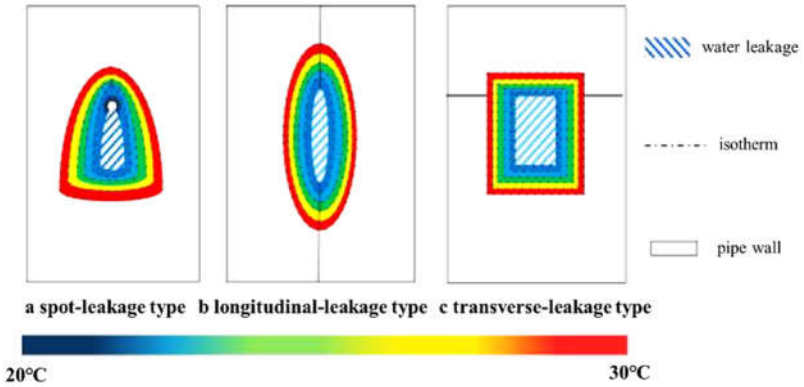

Fig. 14. Temperature distribution of different leakage types [78].

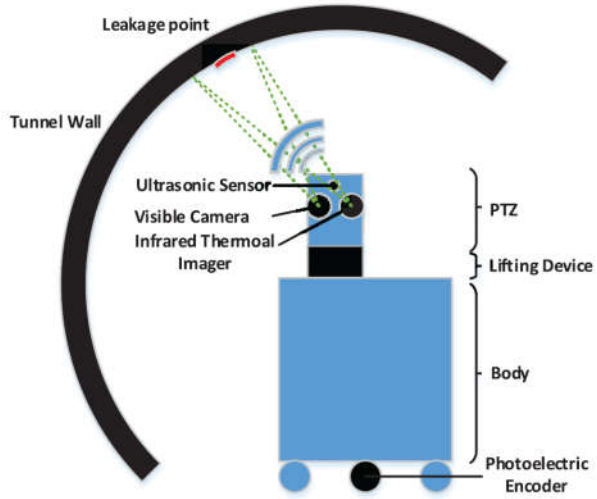

Fig. 15. The cable tunnel inspection system with an infrared camera [79].

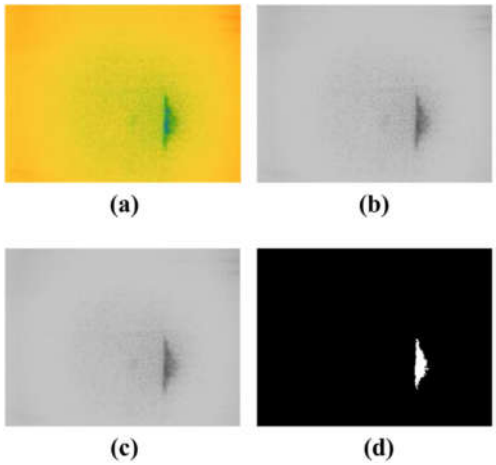

Fig. 16. (a) infrared image of tunnel lining leakage; (b) gray processing; (c) filtering; (d) binarization and threshold segmentation [79].

Due to the difference in absorption of infrared laser light between the moist and dry lining, the lower laser intensity indicates the suspected leakage point [78]. Mobile laser scanning (MLS) can be used to achieve fast and high-precision acquisition of tunnel lining surface information, the threshold-based segmentation is then performed on the laser intensity data to obtain the leakage points. **Fig. 17** shows the composition of the MLS system GRP5000 [80]. The MLS vehicle was integrated with a laser scanner, computer, battery, odometer, and other instruments. Considering that the appendages in the tunnel may have the same laser reflectivity as the leakage area, some auxiliary methods were used to remove these interferences. In the aforementioned work of Yu et al. [78], threshold segmentation based on the Otsu method was used to obtain the suspected water leakage

from the laser intensity image of the tunnel, and the area measurement was performed after confirming the actual water leakage using an infrared camera. Xu et al. [81] used terrestrial laser scanning (TLS) to obtain the 3D point cloud and laser intensity data. The correction of laser intensity data eliminated the effects of distance and incident angle. They also considered the impact of the surface roughness of the tunnel. Similarly, a threshold-based method was applied to segment the leakage area from the intensity image. Afterward, the appendages were removed based on the 3D point cloud. The above-mentioned works provide fast, accurate, and robust leakage detection by combining laser intensity data with other methods and using a threshold algorithm. In recent years, some applications of deep learning methods in processing laser images have also been carried out for leakage detection. Huang et al. [80] used Mask R-CNN to detect water leakage after converting the 3D point cloud into a 2D grayscale image, whose gray value of each pixel was derived from the average laser intensity in the grid. A new triangular mesh method was then proposed to reconstruct the 3D model of the tunnel lining to show detailed leakage information. Cheng et al. [82] proposed an improved FCN-based VGG-19 to achieve automatic leakage segmentation in the corrected laser intensity images. This rapid, high-precision and robust method was not affected by tunnel attachments, but the quantitative assessment of leakage was not available. In summary, the significant advantages of laser intensity-based leakage detection are high integration, high precision, fast tunnel scanning and no dependence on visible light illumination. However, in comparison to infrared thermography, leakage diagnosis based on laser scanning requires more complex data correction and detection algorithms and may require cooperation with other sensors.

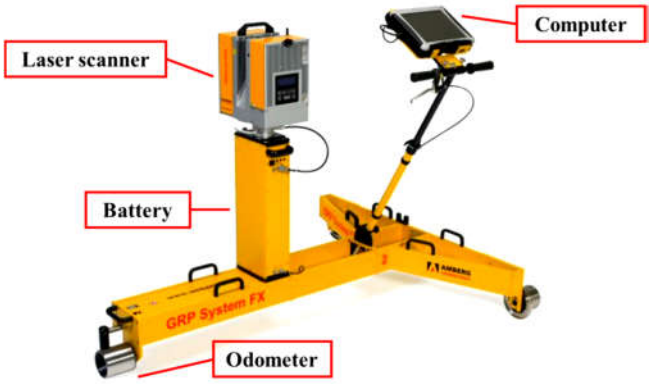

Fig. 17. The MLS system GRP5000 [80].

Apart from the visual characteristics, other traits of the moist concrete, such as electromagnetic

wave velocity, conductivity, and relative permittivity, have also undergone significant changes with the existence of leakage [21,83,84]. These characteristics can be used to inspect leakage inside the lining. Lin et al. [83] proposed an alternative method for detecting tunnel lining leakage using GPR. The sensitivity of GPR to leakage was demonstrated through forward modeling and back projection imaging. Detailed interpretation criteria for tunnel lining defects, including water-conducting fissures, were also established. In addition, the moisture content in the structure could be imaged through conductivity measurement of the dielectric parameters [21]. Sensing the change in relative permittivity could also be used for leakage inspection, such as the ECT technique. Voss et al. [84] investigated the ECT method for monitoring unsaturated moisture flow in cement-based materials. Three cylindrical specimens with different water-cement mass ratios were used as the experimental objects, and the ECT reconstructed the relative permittivity distribution, which reflected the inside moisture ingress, as shown in **Fig. 18**. These NDT methods for investigating leakage and moisture distribution inside the lining are valuable and promising in field applications. However, only qualitative detection results can be obtained because the resolution of them in leakage detection is relatively low when compared with vision-based methods.

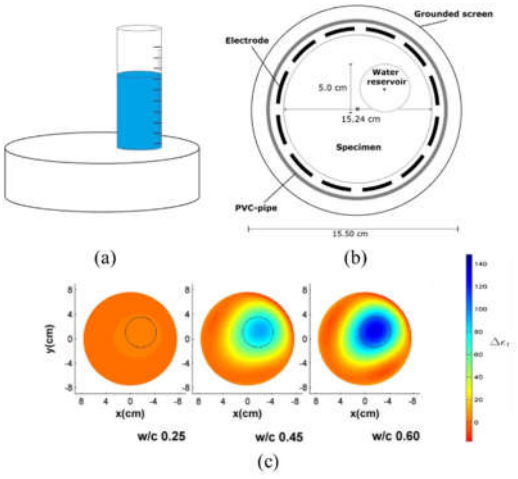

Fig. 18. ECT experiment: (a) a specimen and a water reservoir, (b) top view of the ECT experimental set-up and (c) ECT reconstructions of three specimens with different water-cement mass ratios after 48 hours [84]**.**

To summarize the NDT methods for tunnel leakage detection, image processing and deep learning methods based on visible images remain the most common and attractive methods. Infrared and laser intensity-based methods are gaining more attention due to their suitability and

effectiveness for leakage detection. However, their robustness needs improvement, and the quantitative results are not precise enough. In addition to image-based methods, penetrating NDT methods, such as radar and electrical tomography, are also used for inspecting internal leakage. Some of these methods are still in the laboratory research stage and have not been applied in the field yet.

2.3 Voids

Voids behind tunnel linings are one of the main causes of cracks and leakages [13]. In addition, the lining loses contact with the surrounding rocks due to the existence of voids, resulting in possible structural damage. Therefore, detecting voids and performing timely retrofitting are essential for tunnel structure safety. However, voids are difficult to detect since they are not directly visible on the surface, and vision-based methods are ineffective in detecting them. Therefore, NDT methods with penetrating capabilities provide the possibility for void detection [17].

Investigating the internal state by coring is one of the most common methods in geological surveys [22]. Core samples extracted from tunnel linings allow for direct observation of the internal structure and evaluation of the internal damage. However, coring can only be used at test points, and the full internal status of the object cannot be reflected. Additionally, coring may have negative effects on the structure [85]. Therefore, more efficient, fast, and non-destructive methods have been developed to inspect the internal status of tunnel linings.

GPR is currently the most mature and popular technique for the rapid detection of voids within or behind tunnel linings. **Fig. 19** shows a typical GPR profile. In the tunnel lining reinforced concrete cavity model (**Fig. 19 (a)**), two cavities are located at a depth of 0.35m, and a layer of steel mesh is at a depth of 0.1m. The GPR forward profile is effectively imaged in **Fig. 19 (b)** [85]. The location of the steel mesh and the two cavities can be easily distinguished. In the field of tunnel NDT inspection, air-coupled GPR data is recommended to be collected first, and the area of interest can then be tested in detail by ground-coupled GPR and other in-situ detection methods [22]. Air-coupled GPR, mounted on a rapid detection vehicle, generally operates at a high frequency, resulting in better resolution but shallow penetration depth. In the research of Alani and Tosti [86], the differences between the two operating frequencies of GPR were investigated, and their findings suggested the use of multiple operating frequencies to obtain information about targets located at

different depths with different shapes, dimensions, and constituent materials. GPR requires complex data interpretation, which has a significant impact on detection accuracy. Therefore, research on detecting tunnel lining voids primarily focuses on methods for data interpretation, particularly FDTD techniques [58,59,85,87], and the latest deep learning methods [88,89]. Yu et al. [87] used GPR to investigate the thickness of the grouting layer and the defects in it, where FDTD was applied for data interpretation. In the field measurements, several grouting anomalies, including voids, were successfully detected by analyzing the waveform characteristics of the GPR. The detection results could be used as a reference for subsequent repairs. Lyu et al. [85] applied the reverse-time migration (RTM) algorithm, combined with the FDTD method and the normalized cross-correlation imaging condition, to detect the tunnel lining cavities. The RTM algorithm has been proven to make sense in highlighting the effective signal and suppressing the interference. Qin et al. [88] introduced an automatic detection method based on Mask R-CNN for accurately identifying steel ribs, voids, and initial linings from GPR images. To improve recognition accuracy, the researchers used the FDTD and deep convolutional generative adversarial network (DCGAN) methods for GPR data augmentation. Liu et al. [89] proposed GPRInvNet, a deep neural network that directly constructs relative permittivity maps from GPR B-scan data. The trace-to-trace encoder of GPRInvNet effectively fused information from neighboring GPR traces and automatically extracted key features from the B-Scan data. GPRInvNet performed well in the inversion of defects when applied to real GPR data processing. In the field of engineering applications, Zan et al. [90] developed a high-speed monitoring system equipped with a non-contact air-coupled GPR. The system efficiently worked without interfering with railway operations. The system shown in **Fig. 20** consisted of a rail mobile vehicle, air-launched antennas, and matching control and imaging units. For GPR, high resolution implied weak penetration, which meant that selecting the frequency involved making a trade-off between these two contradictory properties. Furthermore, data interpretation posed its own set of challenges. However, GPR is still recommended in many retrofitting manuals because of its maturity and reliability.

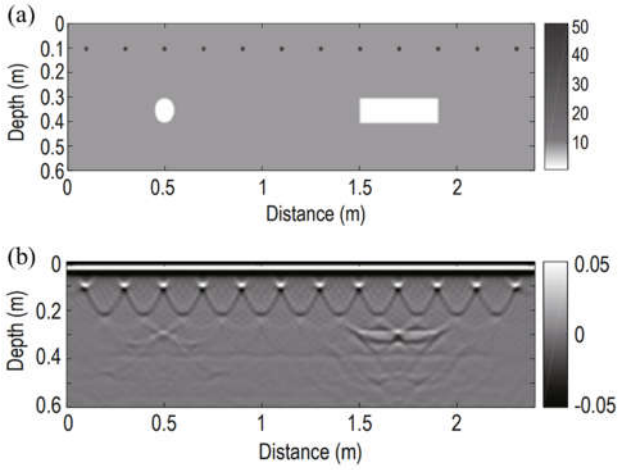

Fig. 19. (a) Schematic map of GPR model, (b) Reverse-time migration profiles of tunnel lining cavity model [85]**.**

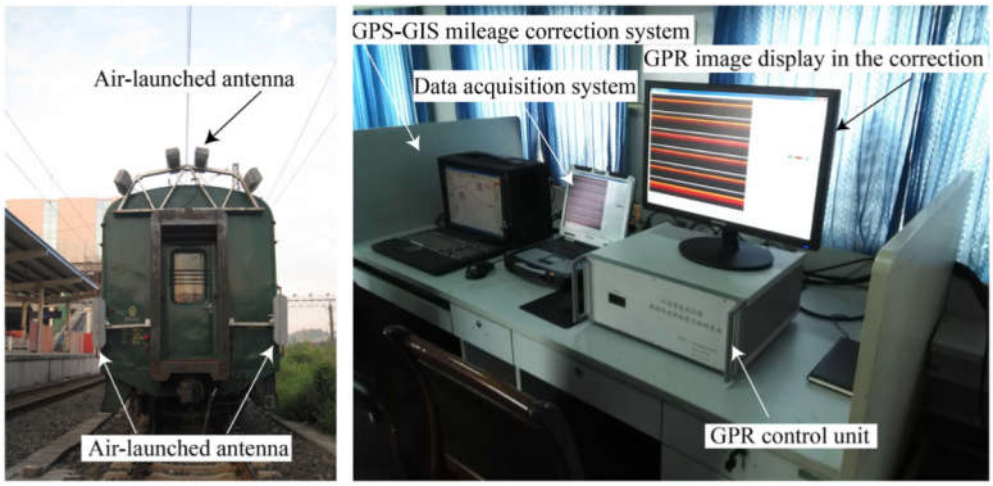

Fig. 20. Vehicle-mounted GPR system [90]**.**

Another type of radar used in engineering inspection is the transient electromagnetic radar (TER), which is based on the difference in electrical resistivity of materials. The principle of the transient electromagnetic method (TEM) is shown in **Fig. 21,** where TER identifies resistivity information by applying a pulsed current to the transmitting coil (Tx-loop in **Fig. 21**) to create a transient electromagnetic field and receiving the secondary induced electromagnetic field by the receiving coil (Rx-coil in **Fig. 21**) from the subsurface layers [91]. By analyzing the received electromagnetic field, the electrical resistivity and parameter information of the subsurface can be measured. Ye and Ye [91] developed a TER (**Fig. 22**) to detect the voids behind tunnel linings and

compared the results with GPR. The steep curve and high resistance in TER images revealed the existence of voids. During field testing, TER observed signals of voids that were not found in GPR images, and subsequent drilling tests confirmed their existence. TER is suitable for tunnel inspection fields because of its deeper detection depth and higher sensitivity to low-resistance materials, such as water, concrete, and rebar. Therefore, TER can make up for the deficiencies of GPR and be applied in the engineering inspection field [92]. The combination of TER and GPR can provide new approaches for voids inspection.

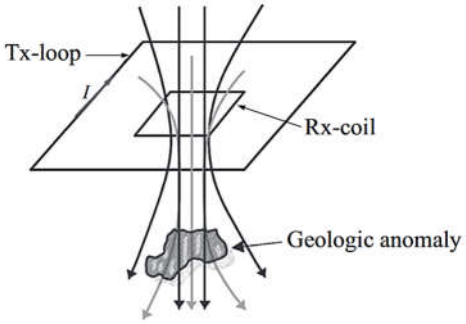

Fig. 21. Principle of the TEM [91]**.**

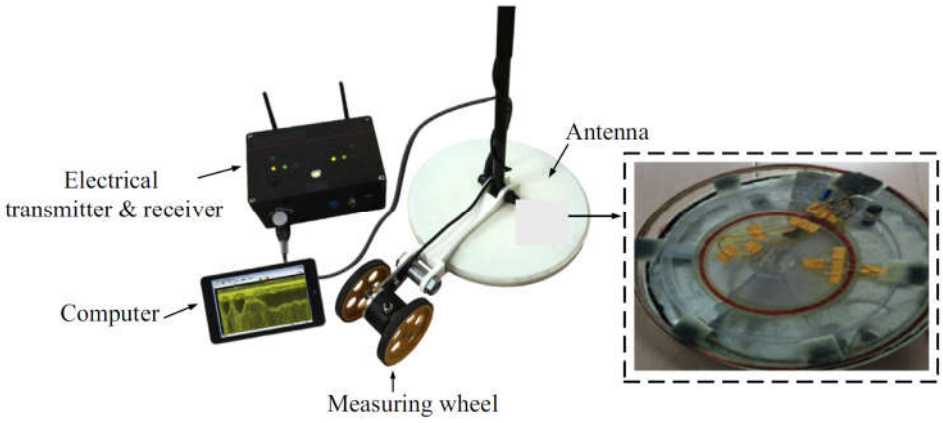

Fig. 22. TER system components [91]**.**

Acoustic techniques are important for detecting voids behind linings [23,93–98]. Impact-echo, an acoustic NDT method, is a reliable and widely used method for detecting internal defects in concrete. Carino [93] summarized the theory, numerical simulation, experimental verification, and field demonstrations of the impact-echo method. Cao et al. [94] compared several signal analysis approaches used in the impact-echo method for detecting voids behind linings. The experiment

showed that the wavelet analysis can provide better energy distribution, and the dynamic stiffness method can determine the location of voids. Acoustic/ultrasonic tomography and impulse response techniques can also detect and locate large air voids [23]. Acoustic tomography, such as elastic wave tomography (acoustic emission tomography), can visualize the wave velocity field distribution of large concrete structures [95,96]. In practical tunnel inspection applications, a portable ultrasonic tomography scanner was used to detect defects behind the linings. White [97] evaluated a phased-array ultrasonic tomography system (**Fig. 23**) and carried out a series of experiments on specimens and in the field. The ultrasonic tomography images of the simulated voids in concrete slabs are shown in **Fig. 24.** The system successfully detected and located air-filled and water-filled voids in the field test. To enhance the penetration and resolution, the synthetic aperture focusing technique (SAFT), total focusing method (TFM), and phased array (PA) technique have been applied to ultrasonic tomography [98]. However, acoustic-related techniques are still used as a complement to GPR. Ultrasonic tomography devices are used after selecting the suspected defective region by air-coupled GPR or other methods suitable for rapid detection.

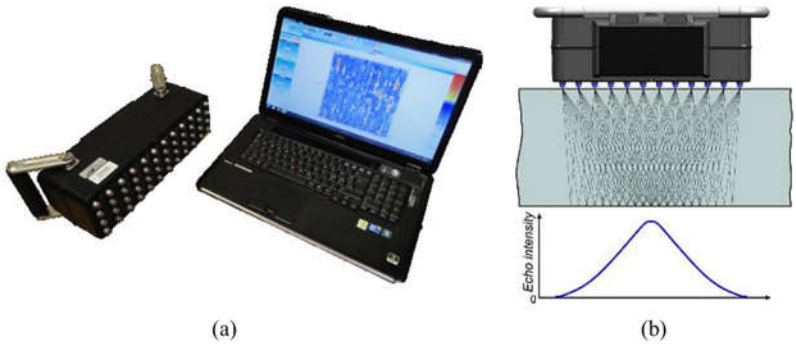

Fig. 23. (a) The A1040 MIRA system and (b) the transmission/reception of acoustic waves and corresponding echo intensity [97]**.**

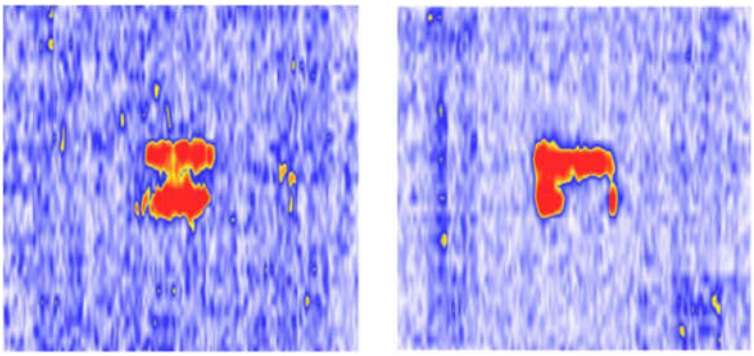

Fig. 24. Typical C-scans for simulated defects in concrete slabs: (a) air-filled void, (b) water-filled void [97]**.**

In addition to ultrasonic tomography, other imaging and tomography techniques have also shown potential for void detection. As aforementioned, passive infrared thermography has limitations, such as the requirement for temperature difference and restricted detection depth. In the work of Konishi et al. [99], it was demonstrated that the passive approach had a higher detection rate if the concrete surface temperature was 0.35 ℃ higher than the air temperature in the tunnel. Therefore, the temperature condition must be strictly met for tunnel inspection using a passive approach, making it relatively restricted. Afshani et al. [100] discussed the heat transfer in concrete, tunnel air, and air inside voids, considering the effects of void type (open or closed), void depth, and temperature differences. Another conclusion was that the temperature difference between the concrete surface and the air in the tunnel of more than 0.35 ℃ was useful for detecting voids of less than 30 mm in depth. Compared with the passive approach, the active approach has more flexible configurations and better detection capabilities, but it requires longer heating and recording times due to the low thermal diffusivities of the materials [101]. Electrical tomography may also have a position in void detection of tunnel linings in the future. It has been used to inspect the internal condition of the concrete. In the experiments by Karhunen et al. [70], the ERT technique was used to reconstruct the conductivity distribution of a concrete specimen with a polyurethane which was simulated as an electrically insulated space. But these experiments in the laboratory were limited in field detection, specifically in strict electrical coupling with the specimen surface, which posed a challenge for rapid detection in the field. In addition, radiography, as a traditional NDT technique, can also be used to detect internal defects in materials. The absorption of radiation depends on the

density and thickness of the material [21]. Cui et al. [102] tested and compared two X-ray backscatter single-side imaging systems. The image systems were able to detect the defects in the concrete under the cover with high resolution. Due to the fact that tunnel lining can only be accessed from one side, radiography is often employed to assess components rather than massive concrete structures like tunnel lining. Another limitation is the radiation of the rays is a threat to the health of engineers/technicians. The X-rays, gamma rays, and neutron rays have a strong penetrating ability due to their extremely short wavelength, necessitating the use of radiation protection in the field.

The invisible property of the voids behind the tunnel lining makes them more difficult to be detected. Typically, rapid air-coupled GPR scanning and manual inspection are used to detect voids initially, followed by other methods such as ground-coupled GPR, impact-echo, ultrasonic tomography, and infrared thermography to collect supplementary information. However, for the newly introduced techniques such as TER, electrical tomography, and radiography, research on this topic is still limited. Therefore, further studies are required to optimize the utilization of these methods and devise an appropriate detection scheme for voids inspection.

2.4 Summary and outlook

Among the three presented defects, cracks are the most concerning issue when it comes to lining deterioration, and their detection methods attract the most attention. For crack detection, vision-based methods are the most widely used, while other detection methods are used as auxiliary. Similarly, visible light-based detection is commonly used for identifying leakage. However, the visible light-based method requires even illumination and is susceptible to interference from objects with the same visual characteristics as the targeted defect, such as stains or tunnel attachments. Therefore, two alternative methods based on infrared images and laser intensity images have been proposed for vision-based detection of cracks or leakage. Voids are located behind the tunnel lining, rendering vision-based methods ineffective. GPR, one of the traditional NDT techniques, is actively used in internal defect inspection like void detection due to its relatively strong penetration ability. These methods can be integrated to achieve more comprehensive inspection, including obtaining the type, location, and size information of defects. For in situ measurements, acoustic tomography techniques are also typically used for internal inspection. In addition, other acoustic techniques,

such as TOFD and SWT, have been proposed to achieve quantitative detection of defects. **Table 1** provides a detailed summary and comparison of the conventional NDT methods for tunnel lining defects.

Although great progress has been made in the detection methods of tunnel linings over the last few decades, the conventional methods still cannot satisfy the increasing requirements of practical applications. Future work may focus on the following points:

1) Different methods can provide different types of defect information, such as location, size, and type, which can be integrated to implement fusion and provide better performance of defect detection. Multi-sensor systems equipped with advanced data fusion algorithms are to be developed to implement the complementarity of different detection methods.

2) The development of artificial intelligence has brought a new dawn for smart sensing and intelligent construction. As the current small-scale defect datasets remain a limitation of learning-based detection methods, the establishment of big datasets will be another focus of future work, either by collecting real-case data with known labels or by developing super-accurate simulation models to generate close-to-reality data. Besides, introducing advanced technology such as expert systems to post-process the results of learning-based black-box methods may be beneficial in making the results more explainable.

3) With the development of robotics, integrated mobile inspection has attracted attention. Tunnel inspection is in great demand and with a large workload, especially for large-scale tunnels. That emphasizes the urgent need for real-time mobile tunnel inspection. Therefore, developing high-efficiency, intelligent, and robust mobile devices or robots that integrate advanced technologies is also an important point of further research.

1 **Table 1 NDT methods for detecting tunnel linings defects**

Method	Targeted defects	Object detected	Characteristics	Advantages	Disadvantages
Manual visual inspection	Cracks Leakage	Surface conditions	Surface status; qualitative	1) Simple; 2) Good applicability; 3) Low technical requirements;	1) Inefficient and inaccurate; 2) Subjective and experience-based; 3) Dangerous; 4) Difficult to integrate information;
Visual inspection	Cracks [47–55]; Leakage [46,51,55,73,75, 76]	Visual characteristics of defects	Surface status; qualitative or quantitative	1) Quick; 2) Standardized; 3) Easy to use; 4) System integrated;	1) Not entirely 2) Accurate; 3) Environmental constraints; 4) Require adequate and even illumination; 5) Require device and algorithms; 6) High cost;
Infrared thermography	Leakage [31,77–79]; Voids [99,100]	The temperature difference between defect area and background	Surface or internal status; qualitative or quantitative	1) Quick; 2) Relatively accurate; 3) Less affected by uneven illumination and surface stains or attachments in the tunnel;	1) Complex image processing; 2) Low resolution of infrared images; 3) Influenced by infrared noise; 4) Limited detection depth by passive method;
Radar	Cracks [58–61]; leakage [83]; voids [58,59,85–91]	Electromagnetic wave velocity; transmission and reflection on the interface	Internal status; qualitative	1) Quick; 2) Continuous; 3) Good penetration; 4) Relatively high resolution;	1) Rely on data interpretation; 2) Rely on the selection of antenna frequency and the design of the antenna;
Laser	Leakage [78,80–82]	Laser intensity difference between leakage area and background	Surface status; qualitative or quantitative	1) Quick; 2) Accurate; 3) No dependence on visible light illumination;	1) More complex data processing; 2) Easy to be affected by tunnel appendages; 3) High cost;

Acoustic techniques	Cracks [62–69]; voids [94–98]	Transmission, reflection, refraction and diffraction of sonic/ultrasonic wave	Internal status; qualitative or quantitative	1) Low cost; 2) Tomography possible;	1) Relatively slow; 2) Low penetration depth; 3) Rely on data interpretation; 4) Mostly require good coupling;
Electrical tomography	Cracks [70,71]; leakage [84]; voids [70]	Electrical impedance distribution	Internal status; qualitative	1) Low cost; 2) Good real-time performance; 3) Visualization;	1) Low penetration depth; 2) Relatively low resolution; 3) Rely on data interpretation;
Radiography	Voids [102]	Attenuation of rays in concrete	Internal status; Qualitative	1) Extremely strong penetration ability; 2) High resolution; 3) Visualization;	1) High cost; 2) Radiation hazard; 3) Radioactive source required;

3. Evaluation methods of tunnel lining

Existing tunnels may suffer from a variety of problems over time [103]. These issues may impair the service of tunnels and cause deterioration in the performance of structures [104]. Therefore, it is necessary to assess the serviceability conditions of the tunnel linings. Based on the results obtained by NDT methods for tunnel lining defects, structural health evaluation of the tunnel is followed. This section provides an overview of typical evaluation methods and summarizes the future research that needs to be addressed.

The evaluation process of tunnels is illustrated in **Fig. 25.** The overall condition of the tunnel can be evaluated by considering its different subunits. Based on detection data and evaluation methods of each subunit, evaluation results can be obtained against evaluation criteria. Routine maintenance or retrofitting in the future will depend on the final evaluation result.

With the increase of tunnels, the Federal Highway Administration published a manual [105] that provided useful guidance on the evaluation of operating tunnels to assess aged railway tunnel linings. Park et al. [44] investigated the evaluation of tunnel defects. Although the evaluation criteria were based on expert opinion and experience, the evaluation results in their research were objective because quantitative evaluation methods were used. To reduce the subjectivity in tunnel evaluation, scientific and rational methods for evaluating the condition of tunnel linings are essential [106]. Meanwhile, mathematical models and artificial intelligence techniques are gradually developed or

introduced to evaluate the condition of tunnels more accurately. Thus, existing evaluation methods can be categorized into three types, including normative assessment method, evaluation using mathematical models, and evaluation using artificial intelligence technology.

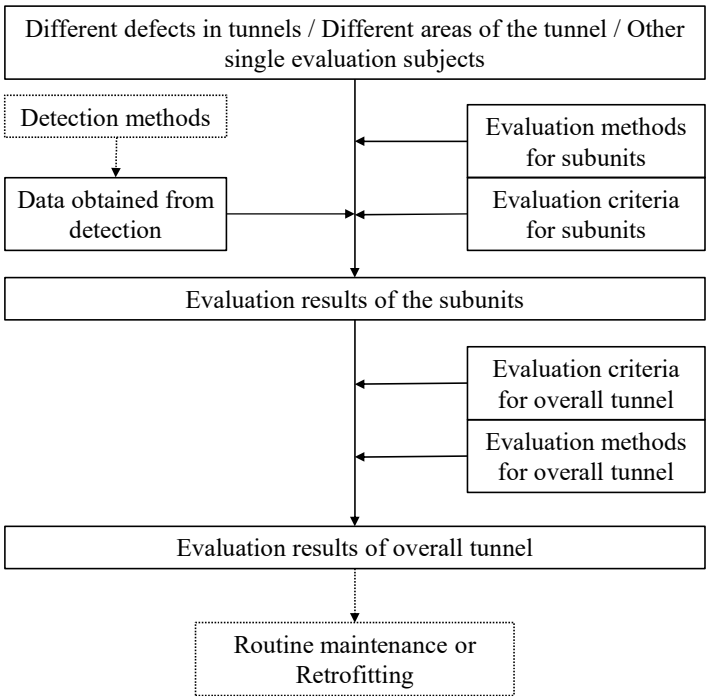

Fig. 25. Diagram of the evaluation process.

3.1 Normative assessment method

The normative assessment method is primarily based on the relevant specifications. This assessment method takes a wide range of factors into account and a rapid evaluation can be achieved. The normative assessment method can directly and quickly assess the overall condition of a tunnel, as well as the assessment of localised tunnel defects. For example, the general technical situations of road tunnels can be assessed in accordance with the Technical Specifications of Retrofitting for Highway Tunnel [107]. Through this method, the civil structure can be assessed from three aspects: the electrical and mechanical facilities, the civil engineering facilities, and other engineering facilities. The level-by-level evaluation of the normative assessment method is summarized in **Fig. 26**. The assessment of the civil structure of the tunnel usually starts with a technical condition score according to the following equation:

$$JGCI = 100 \cdot \left[1 - \frac{1}{4}\sum_{i=1}^{n}\left(JGCI_i \times \frac{\omega_i}{\sum_{i=1}^{n}\omega_i}\right)\right] \quad (3)$$

where ω_i is the weight, $JGCI_i$ is the condition value of the subunit and $JGCI$ is the overall condition value. Then the civil engineering structures will be categorized according to **Table 2** and **Table 3**. In addition, the specification provides separate assessment methods for localised tunnel defects such as cracks and leakage, with the assessment condition values defined in **Table 4**. The extent of defects can be quantified by condition values in **Table 5** and **Table 6**.

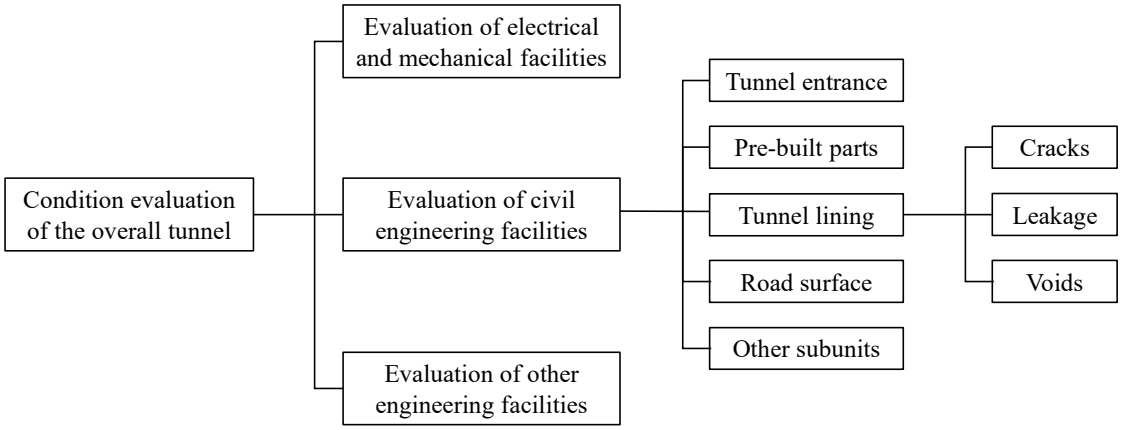

Fig. 26. Diagram of the level-by-level evaluation in the normative assessment method.

Table 2 Threshold values for the classification of the technical condition of civil structures [107]

Technical condition rating	Classification of the technical condition of civil structure				
	Category 1	Category 2	Category 3	Category 4	Category 5
JGCI	⩾85	⩾70，＜85	⩾55，＜70	⩾40，＜55	＜40

Table 3 Classifications of the overall technical status of highway tunnels [107]

Technical condition rating category	Rating category description	
	Civil structure	Electromechanical facilities
Category 1	Intact condition	High integrity rate
Category 2	Minor breakage	Normal integrity rate
Category 3	Moderate breakage	Still operational
Category 4	Severe breakage	Low integrity rate
Category 5	Dangerous condition	——

Table 4 Definition of condition values [107]

Condition value	Evaluation factors		
	Degree of defect	Development trends	Impact on traffic safety and structural safety
0	None or extremely minor	None	No impact
1	Minor	Stable	No impact yet
2	Moderate	Slow	Will impact
3	Severe	Quick	Already impacts
4	Dangerous	Rapid	Severe impacts

Table 5 Evaluation criteria for crack [107]

Structure	Crack width b (mm)		Crack length l (m)		Condition value
	$b > 3$	$b \leqslant 3$	$l > 5$	$l \leqslant 5$	
Lining	√		√		3/4
	√			√	2/3
		√	√		2
		√		√	2

Table 6 Evaluation criteria for water leakage [107]

Structure	Major abnormal conditions	Degree of leakage				Whether it affects traffic		Condition value
		I	II	III	IV	Yes	No	
Arch	Water leakage	√				√		4
			√			√		3
				√		√		2
					√		√	1
	Hanging ice					√		3
							√	1
Side walls	Water leakage	√				√		3
			√			√		2
				√		√		2
					√		√	1
	Hanging ice					√		3
							√	1
Road surface	Sandy outflow					√		3/4
							√	1
	Ponding					√		3/4
							√	1
	Freezing					√		3/4
							√	1

It is also possible to assess the condition of the tunnel using thresholds for tunnel defects or deformations in some specifications, such as the threshold values for tunnel wall convergence recommended in the Standard for Design of Metro [108] and the allowable value for crack widths recommended in the Standard for Design of Shield Tunnel Engineering [109]. However, the inconsistent grading of different defects in the specifications results in the normative assessment method relying significantly on the experience of the experts [26]. To avoid mistakes in the evaluation results due to human subjectivity, the normative assessment method can be combined with the NDT techniques. For example, Lai et al. [28] applied crack width monitoring technology, concrete strength monitoring technology, and electromagnetic wave nondestructive monitoring technology for the evaluation of the overall condition of the tunnel. The detection data obtained from NDT techniques, rather than expert ratings, make the evaluation results more objective. However, incorporating these techniques inevitably increases the cost of the evaluation.

3.2 Evaluation using mathematical models

Mathematical models can be used to evaluate the health condition of the tunnel [26]. Different detection data, such as sensor readings or imaging data, can be transformed by mathematical models into usable data that can be used to derive evaluation results. Crack is one of the most common defects in existing tunnels [2]. As aforementioned, cracks can easily be detected by NDT methods. As a result, some researchers have chosen to use cracks as a primary indicator when assessing the condition of tunnel linings. Shigeta et al. [110] attempted to quantitatively assess the condition of the tunnel lining by collecting crack information from available tunnels. They proposed a Tunnel lining Crack Index (TCI) that took into account the size and distribution of the cracks. The conceptual diagram of TCI is shown in **Fig. 27**. TCI can be calculated based on the crack tensor theory using the following equation:

$$F_{ij} = \frac{1}{A}\sum_{k=1}^{n}\left(t^{(k)}\right)^{\alpha}\left(l^{(k)}\right)^{\beta}\cos\theta_i^{(k)}\cos\theta_j^{(k)} \tag{4}$$

where A is the area of concrete, n is the number of branches of the crack, $l^{(k)}$ is the length of the kth crack, $t^{(k)}$ is the width of the kth crack, $\theta_i^{(k)}$ is the angle between the normal vector of the kth crack and the i-axis, $\theta_j^{(k)}$ is the angle between the normal vector of the kth crack and the j-axis, α

is a factor related to the width of the crack, β is a factor related to the length of the crack. This evaluation method has been widely used [25]. However, this method did not take into account the complexities that arise when cracks intersected with each other and therefore had limitations [25]. At the same time, the uncertainty in the relationship between TCI and the instability of tunnel lining indicated that this method needs further investigation [29].

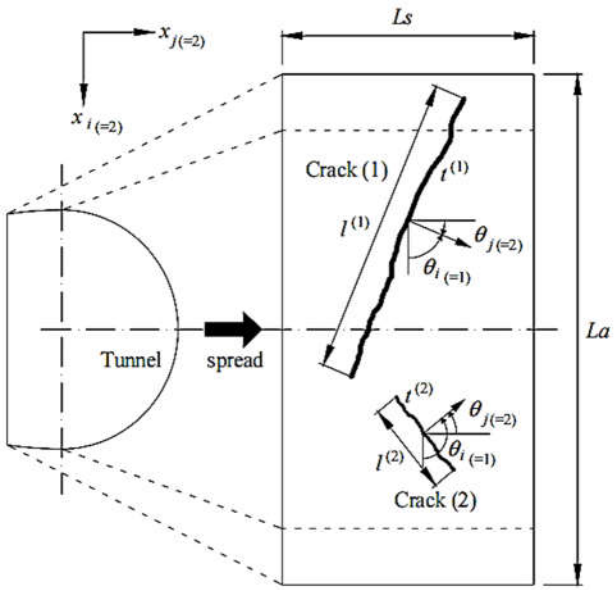

Fig. 27. The conceptual diagram of TCI [29]**.**

The fractal theory could be used to describe the propagation of cracks and the fractal dimension was very effective in characterizing the degree of damage and fragmentation [111,112]. Jiang et al. [25] proposed a Box-Counting method for assessing the health condition of tunnel linings based on fractal dimension theory. The local surface of the lining with cracks was assumed to be an expansion plane in this method. The plane could be divided into equally spaced grids of scale *r* and the number of grids occupied by the cracks in the plane was *N(r)*. Then the fractal dimension *D* could be obtained by the following equation:

$$D = \lim_{r \to 0} \frac{log\, N(r)}{log\left(\frac{1}{r}\right)} \tag{5}$$

A schematic diagram of the calculation is shown in **Fig. 28**. The evaluation results were validated by TCI. The correlation between the fractal dimension *D* and the TCI is shown in **Fig. 29**. The fractal dimension took into account the density, width, and distribution of the cracks. Therefore, this

method was theoretically more reasonable than TCI. However, the fractal dimension possessed the same disadvantages as the TCI evaluation method, such as the high cost of the evaluation process and the inadequacy of the evaluation indicators.

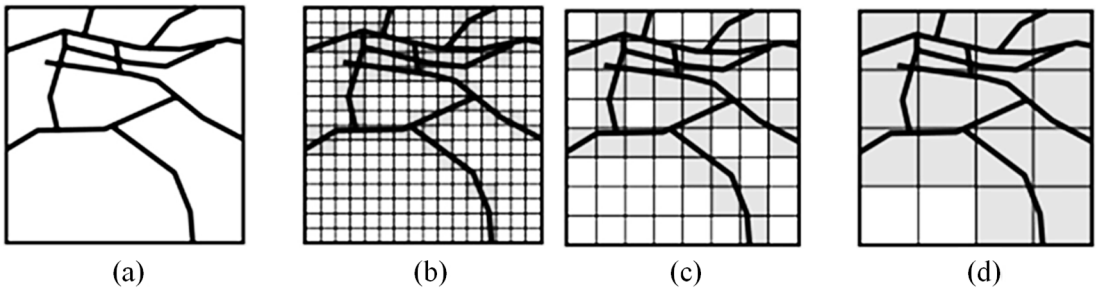

Fig. 28. Schematic diagram of the Box-Counting method. (a) Crack image; (b) $r = 1, N(r) = 86$; (c) $r = 2, N(r) = 34$; (d) $r = 4, N(r) = 14$ [25].

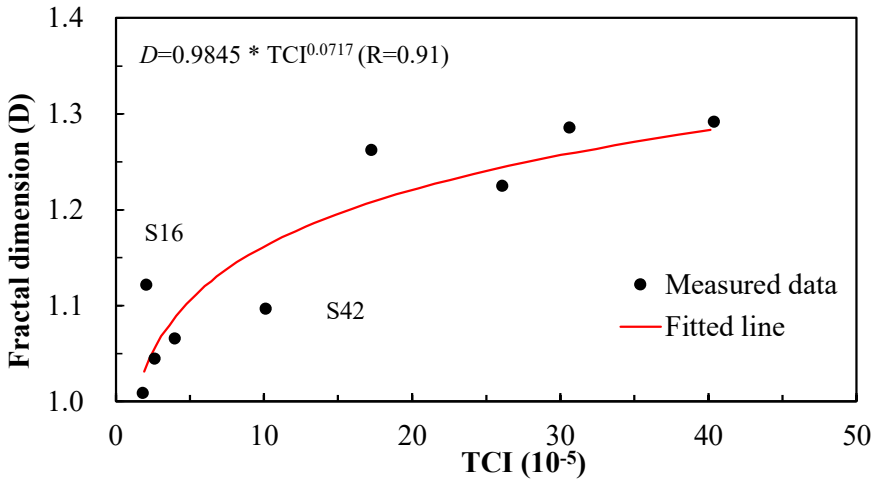

Fig. 29. Correlation between fractal dimension and TCI [25].

Yuan et al. [113] proposed a comprehensive evaluation framework for tunnels based on the principle of limit state design, in which limit state functions were used. The methodology classified the service state of the tunnel into five levels (**Fig. 30**). Based on the measured data, a limit state function was used to determine the level of service state of the component. The evaluation framework started from the structural components to the individual lining rings, and finally to the overall condition of the tunnel. **Fig. 31** shows the assessment framework. Li et al. [26] investigated a similar classification for the service state of the tunnel but proposed a different mathematical

model called the tunnel serviceability index (TSI) formula. The TSI formula is as follows:

$$TSI = A_1\sqrt{s_{ave}} + A_2 s_{diff\,ave} + B_1 c_{ave} + C_1 d_l + C_2 d_c + C_3 d_s + C \quad (6)$$

where s_{ave}, $s_{diff\,ave}$, c_{ave}, d_l, d_c and d_s are measurable variables, s_{ave} is the average relative settlement, $s_{diff\,ave}$ is the average differential settlement, c_{ave} is the average convergence ratio, d_l is the total water leakage area, d_c is the total cracking length and d_s is the total spalling area. A_1, A_2, B_1, C_1, C_2, C_3 and C are coefficients estimated by partial least squares regression and linear transformation.

Further research on the TSI was conducted by Lin et al. [114], who compared the assessment results of the TSI formula with those obtained from the normative assessment method. Their research showed that the TSI method was more conservative. Additionally, Andreotti et al. [115] proposed a cyclic model for longitudinal joints that considers the effect of cyclic loads, and Lin et al. [106] proposed a tunnel structural toughness model that considers multiple disturbances. It was shown that such models could accurately assess the condition of tunnels in earthquake-prone areas.

In general, the application of mathematical theory to the condition evaluation of tunnel linings can lead to more accurate results, but high-quality data from the detection methods are required to improve the quality of evaluation results.

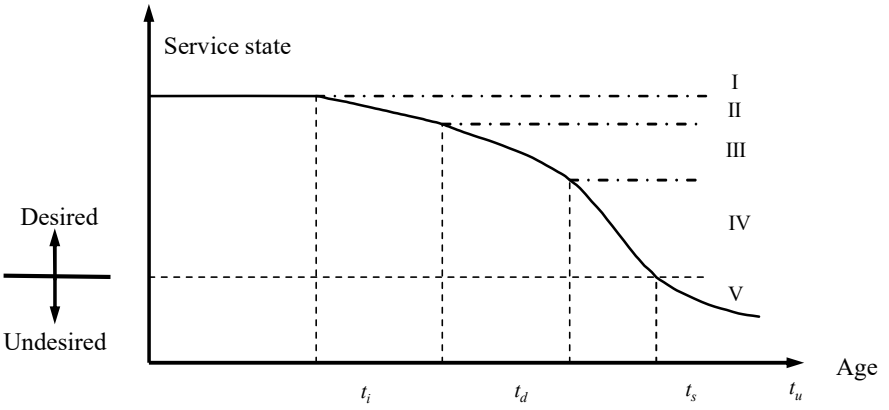

t_i - Operational duration to the initial of degradation; t_d - Operational duration to durability limit state; t_s - Operational duration to availability limit state; t_u - Operational duration to ultimate limit state.

I - Suitable state; II - Degraded state; III - Deteriorated state;
IV - Unavailable state; V - Unstable state.

Fig. 30. Evolution in service state [113]**.**

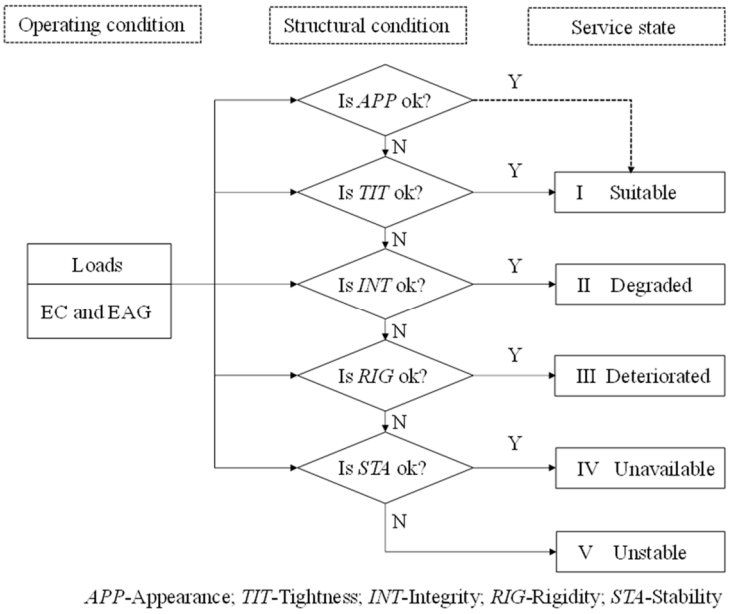

Fig. 31. Flowchart in assessment [113]**.**

3.3 Evaluation using artificial intelligence technology

With the development of artificial intelligence technology, some researchers started to apply it to the assessment of tunnel conditions. Zhang et al. [116] proposed a dynamic evaluation method for tunnel performance in which Knowledge Graph was used to integrate data. Although the dynamic evaluation model based on Knowledge Graphs was a new evaluation method, it was still based on the static expert rating method. Zhu et al. [30] proposed a new assessment method via cloud model-based random forests (CRFs), with the evaluation workflow shown in **Fig. 32**. The method included supervised and semi-supervised machine learning algorithms. The two algorithms could effectively deal with inconsistent data and limited data respectively. The evaluation method could be further improved with the incorporation of more accurate and numerous data. In addition, Rafiei and Adeli [117] proposed an unsupervised learning model for the condition assessment of large infrastructure systems, which involved machine learning techniques. These approaches can be a valuable reference for tunnel condition assessment. With the development of automatic detection technologies as demonstrated in **Section 2**, it is becoming easier to quickly obtain data to evaluate the condition of tunnel linings [118–120]. Artificial intelligence technology has advantages in data processing. The use of artificial intelligence technology in the condition evaluation of tunnel linings

can lead to improved efficiency and accuracy [24]. However, it is difficult to develop a sufficiently large dataset to cover all real-case states of the tunnels during ageing and deterioration, as well as to obtain accurate labels of all the samples in the datasets.

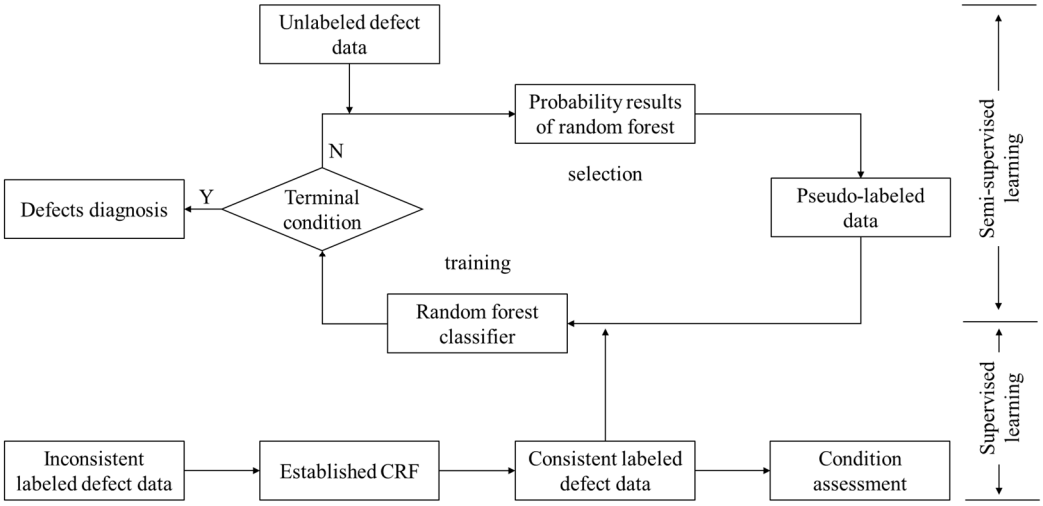

Fig. 32. Schematic illustration of the cloud model-based random forests [30]**.**

3.4 Methodology comparisons and perspectives

The normative assessment method evaluates the tunnels in a relatively comprehensive way as it takes into account not only the structural performance but also other facilities in the tunnels [107]. The method also allows for rapid assessment, which is essential in the case of an unexpected event. However, the method requires the involvement of experts in the assessment. That means the results obtained from the normative assessment method depend on the experts' experience, which is inevitably more subjective. When evaluating the condition of tunnel linings, mathematical models can be applied to different types of damage, but they ignore the correlation between different defects [26]. Artificial intelligence technology has excellent potential in structural condition evaluation, especially for data processing and evaluation with the inputs of multiple detection methods. Such evaluation methods usually do not require supervision, especially deep-learning methods, because they extract the features/information automatically [24]. However, establishing large and comprehensive datasets with accurate labels is still challenging.

In addition to the above three evaluation methods, evaluation can also be conducted based on numerical simulation software [121] and expert rating methods [26]. A summary of these different

evaluation methods is shown in **Table 7**.

Table 7 A summary of the different evaluation methods

Evaluation methods	Characteristics	Advantages	Disadvantages
Normative assessment method [107–109]	Qualitative or semi-quantitative	1) Quick; 2) Economical; 3) high practicality;	1) Accuracy needs to be improved; 2) Generally relying on experts' experience;
Mathematical models [25,26,113,115]	Quantitative	Multiple types of indicators can be considered with a high degree of accuracy.	1) High requirements for evaluation criteria; 2) Complex process of model development and calculation;
Artificial Intelligence Technology [30,117]	Quantitative	1) High precision; 2) Quick;	1) Requires sufficient samples; 2) Algorithm changes can lead to biased results;
Finite element numerical simulation [121–124]	Quantitative	1) Low cost; 2) Good repeatability;	Accuracy in complex environments needs to be improved.
Expert rating methods [31]	Qualitative or semi-quantitative	1) Quick; 2) High practicality;	Evaluation results are subjective.

Future research on tunnel condition evaluation may focus on the following three aspects: 1) Refine the indicators/models to take into account more components and the correlation between different components/defects. 2) Develop real-time assessment methodology to satisfy mobile tunnel inspection, and implement assessment while detecting. 3) Build sufficiently large datasets with accurate reference labels of tunnel states to take full advantage of artificial intelligence technology.

4. Tunnel lining retrofitting methods

The previous sections summarize the types of shield tunnel lining defects and the

corresponding detection and evaluation methods. For various defects, different retrofitting methods can be adopted according to their effects on the performance and safety of the lining. Lining defects that will not affect the ultimate capacity and safety performance of the liner only need normal retrofitting, such as surface damage with inlay repairs [31], as shown in **Fig. 33**. Defects that may pose a significant risk to the structural functions of the tunnel require structural modifications of the lining, and this is the focus in this section. For tunnels in service, retrofitting methods can generally be divided into two categories: internal surface retrofitting and grouting retrofitting, depending on the positions of retrofitting operations [9,125]. Therefore, this section will conduct a review on these retrofitting methods based on the classification of the inner surface retrofitting method and the grouting retrofitting method.

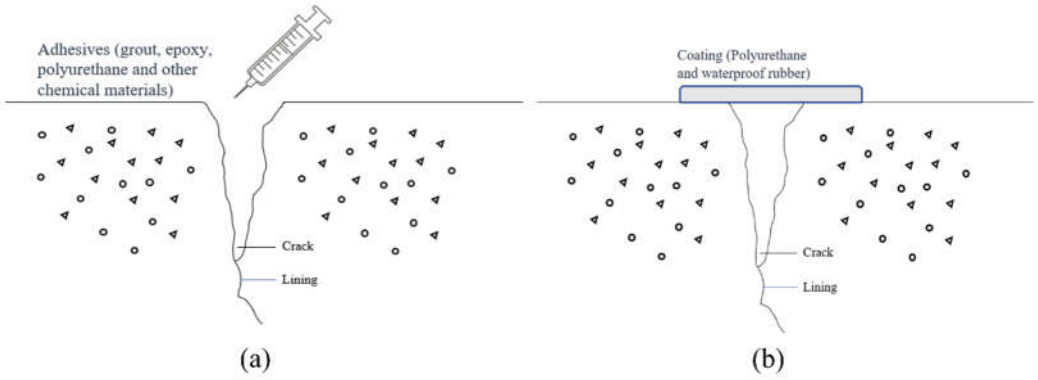

Fig. 33. Inlay repairs: (a) adhesives and (b) coating.

4.1 Internal surface retrofitting

The mechanism for internal surface retrofitting is typically described as reinforcing the tunnel structures from the lining's inner wall. Depending on the retrofitting material, the conventional internal tunnel retrofitting methods often include bonded steel plates, cover-arch reinforcing, and bonded Fiber-Reinforced Plastic (FRP) [32].

4.1.1 Bonded steel plate method

The method using bonded steel plates for tunnel retrofitting was demonstrated by Kiriyama et al. in 2005 [126]. The method works by bonding the steel plates to the defective shield segments using epoxy, which could improve the stiffness and ultimate load carrying capacity of the tunnel structures [127], as shown in **Fig. 34**. Thus, the construction procedures were divided into two stages:

steel plate fixation and epoxy resin infusion. The steel plates were attached along the segmental circumferential midline and then joined together using electric welding. Plug bolts were used to connect the steel plate and the adjacent concrete segment, and finally, epoxy was infused between the two materials. The operations of the bonded steel plates could usually be mechanized, so the construction was quick and efficient [128]. Depending on the area of the bonded steel plate, the method was furtherly classified into full-ring and half-ring steel plate reinforcing methods, as shown in **Fig. 35** [129].

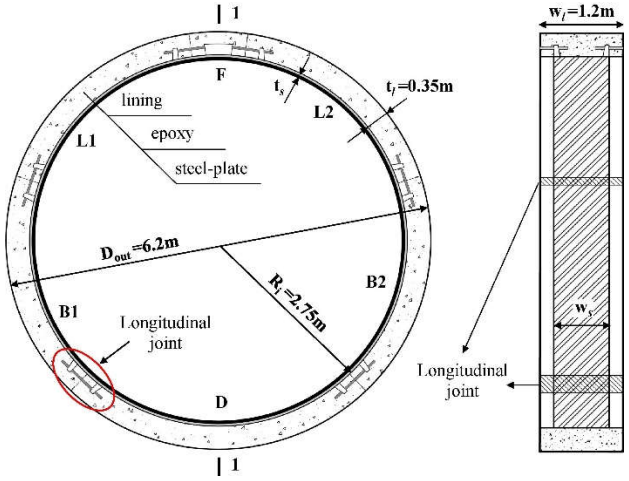

Fig. 34. Bonded steel plate method [127].

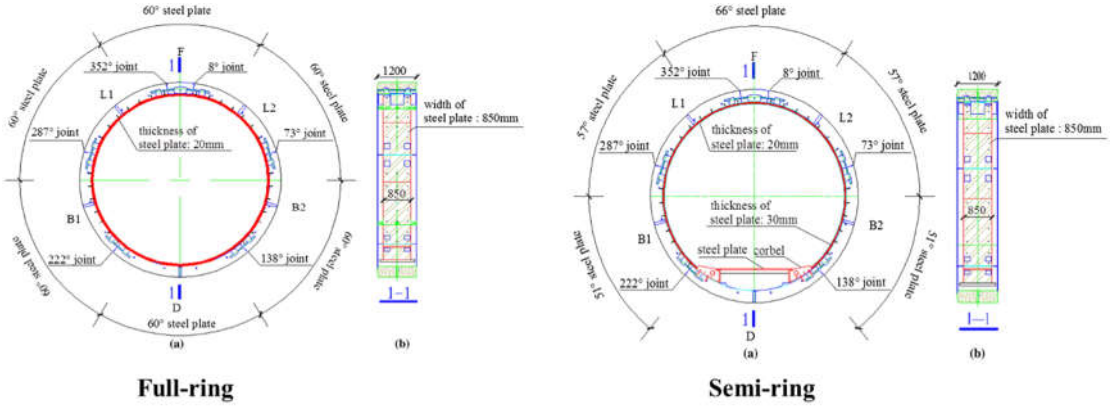

Fig. 35. Shield tunnel reinforced by steel plate: (a) cross-section; (b) longitudinal section [129].

Many researchers have investigated the effectiveness of the bonded steel plate retrofitting method. Chang et al. [130] analyzed the cause of large-scale lateral deformation in shield tunnels and found that the application of the bonded steel plate method could effectively increase tunnel stiffness, even though the deformation was large. To evaluate the load-bearing capacity and the

deformation pattern of the reinforced segments, Liu et al. [129] and Bi et al. [131] conducted full-scale experiments on reinforcing shield tunnels using full and semi-ring inner tensioned steel plates. The results showed that the internal bonded steel method significantly improved the overall stiffness and load-bearing capacity of the shield tunnels. The full-ring strengthening method was found to be more effective than the semi-ring strengthening method. However, the tunnel failure mechanism was not provided in these studies. Additionally, the impact of existing deformation on the performance of post-reinforced linings was not analyzed. Zhai et al. [132] conducted model tests to assess the influence of various levels of deformation on the performance of steel plate reinforced tunnel linings. However, the physical model was simplified and did not accurately represent the actual prototype. Liu et al. [133] demonstrated the efficacy of steel plate retrofitting through model tests on pipe linings with and without retrofitting. Nevertheless, the quantitative damage to the bonding surface and segmental joints has not been thoroughly investigated.

To investigate the structural performance and damage mechanism of shield tunnel lining reinforced with steel plates, Liu et al. [134] established a three-dimensional finite element model based on the structural test of tube lining, reinforced with inner bonded steel rings. Through the finite element analysis and parametric study, the mechanical properties, the deformation characteristics, and the failure modes of tunnel lining reinforced with adhesive steel were discussed. The results demonstrated that the direct cause of the damage to the lining structure after being reinforced with steel plates was the failure of the epoxy resin bond between the steel plates and the lining. It presented a clear brittle behaviour, and conventional deformation monitoring was unable to provide early warnings. Furthermore, several new retrofitting methods for steel members have been proposed by researchers, including bonded corrugated steel [135] and bonded steel pipe concrete [136]. However, it has been observed the strengthened linings were all damaged at the interface, which significantly reduces the retrofitting effectiveness and efficiency. Therefore, it is important to investigate the bonded condition between the steel plates and the liner.

However, the limitations of testing techniques make it challenging to accurately analyze the details of the prototype during physical testing of the model and observe the detailed damage phenomena [137]. Numerical simulations have significant advantages over physical tests when it comes to studying detailed damage characteristics of structures. These simulations offer good

repeatability and analytical capabilities [138]. When simulating the mechanical behavior of steel plate reinforced segment liners, it is crucial to reasonably model the damage behavior at the bonding surface between the steel plate and the segment liner [139]. Sun et al. [140] utilized cohesive contact to model the bonding behavior in ABAQUS. The steel plate reinforcement was also incorporated by adjusting its modulus of elasticity from a low value to a realistic value. The mechanical performance of the cohesive unit was defined using a damage evolution model based on the traction-separation response [141], as depicted in **Fig. 36**.

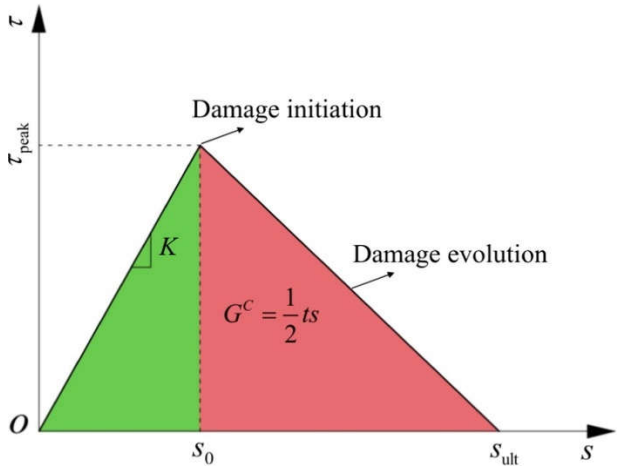

Fig. 36. A model for bond damage evolution based on traction separation response [139]**.**

The definition of the parameters in the figure is shown below: τ is interfacial stress; τ_{peak} is bonding strength; s is the relative displacement between steel plate and lining; s_0 is relative displacement value; s_{ult} is final relative displacement; K is interface stiffness; G^C is the interfacial fracture energy, which is obtained from the following **Eq. (7)** based on the B-K criterion [142,143].

$$G^C = \frac{1}{2}\tau s \tag{7}$$

The mechanical behavior of cohesive elements is divided into three phases.

1) Well-bonded stage. τ and s remain linear, as shown in **Eq. (8)**. No bond damage occurs.

$$\tau = \begin{Bmatrix} \tau_n \\ \tau_{s1} \\ \tau_{s2} \end{Bmatrix} = \begin{bmatrix} K_{nn} & K_{ns1} & K_{ns2} \\ K_{ns1} & K_{s1\,s1} & K_{s1\,s2} \\ K_{ns2} & K_{s1\,s2} & K_{s2\,s2} \end{bmatrix} \begin{Bmatrix} s_n \\ s_{s1} \\ s_{s2} \end{Bmatrix} = Ks \tag{8}$$

where τ_n, τ_{s1} and τ_{s2} are interfacial stress data in different directions, s_n, s_{s1} and s_{s2} are relative displacement data in different directions, K_{ns1}, K_{ns2}, $K_{s1\,s1}$, $K_{s1\,s2}$ and $K_{s2\,s2}$ are the stiffness matrices of the interface.

2) Bond damage phase. Once the interfacial stress value exceeds τ_{peak}, bond damage occurs, as reflected by the decrease in interfacial stress with the development of relative displacement.

3) Bond failure phase. Once the relative displacement value exceeds s_{ult}.

Based on the theory above, Liu et al. [144] developed an analytical solution for predicting interfacial stresses. On this basis, they investigated how the elastic modulus, the thickness of the adhesive layer, and the thin plate affected the quality of the inner surface bonded steel plate reinforcing. However, their study did not take into account the impact of damage to the front section of the reinforcement on the bonding behavior. To address this, Li et al. [139] proposed FEM to accurately simulate the bonding behavior between steel plates and the lining and validated it through detailed physical model tests on tunnels reinforced with steel plates. A series of FEM simulations were conducted for tunnels reinforced under various levels of deformation. The study analyzed the effect of existing structural deformation on the detailed damage mechanisms of the post-reinforced lining under increasing external loads, including the progression of bond damage and the opening and bending stiffness of the joints.

To enhance the bond at the interface, Ren et al. [145] used a large number of chemical anchor bolts instead of structural adhesive to connect the lining to the corrugated steel. Despite some slippage at the bonded interface, the shear capacity from the chemical anchor bolts allowed for the deformation and integration of the structure components, resulting in a final increase in the ultimate load-carrying capacity by 163% to 201%. However, because of the presence of gaps in the retrofitting interface, the method is ineffective in improving the waterproof performance of the tunnel compared to structural adhesive bonding. Liu et al. [146] employed fiber-reinforced concrete as an adhesive material to connect the lining to the retrofitting layer using the bonding effect of cement-based materials, which has the advantage of a fire-resistance and high-temperature resistance. However, the method was restricted to the tensioned region because of the characteristics of the fiber. Therefore, more research is needed to improve the adhesive capacity of the reinforced layer to the lining.

The use of the bonded steel plate method can significantly enhance the overall strength and rigidity of the lining, effectively mitigating tunnel deformation and resolving cracking issues. Additionally, the construction process is straightforward and convenient. However, some challenges need to be addressed [127]:

(1) Higher cost of steel plates and bonding materials.

(2) Increased self-weight of the structure: The addition of steel plates to the structure will add

extra weight, which may affect its stability and safety, especially in the case of overloading or extreme weather conditions.

(3) Additional anchoring measures: To ensure effective bonding between the steel plates and the strengthened elements, a large number of anchoring measures may be required. This can cause secondary damage to the linings and weaken their overall strength.

(4) A lack of efficient bonding materials: The choice of bonding materials is critical to the success of the retrofitting method. The lack of efficient bonding materials that can withstand high loads and stress can reduce the effectiveness of the retrofitting process.

4.1.2 Cover-arch reinforcing

The cover-arch method improves the load-bearing capability of the linings by increasing the cross-sectional areas of the structure [147], as shown in **Fig. 37**. This is achieved by replacing the damaged lining with a concrete structure that is integrated with the original structure. Depending on the cover-arch method can be divided into stacked and separated [148]. The stacked arch involves completely integrating the arch with the original lining, while the separated arch includes a waterproof layer set between the arch and the original lining [149].

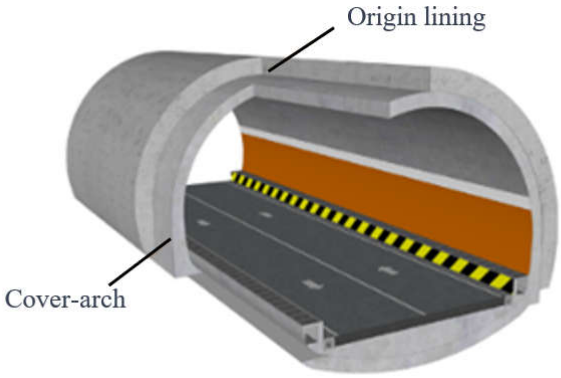

Fig. 37. Cover-arch reinforcing [33]**.**

To investigate the effectiveness of stacked arches reinforcing, Hakoishi et al. [150] experimentally analyzed the deformation process, investigated the failure modes, and measured the ultimate load-carrying capacity of the lining structure after reinforcing the arches in a semi-circular manner, and they observed an increase of the ultimate load-carrying capacity of the lining. However, because the experiment was completely unloaded before reinforcing, it differed considerably from

the actual forces of the lined arch reinforced with cracks. Liu et al. [151,152] used structural experiments, finite element analysis, and field tests to examine the structural behavior and ultimate capacity of the lining reinforced by the stacked arch. They verified the effectiveness of the stacked arch reinforcement and investigated the structural behavior of stacked arch reinforcement in various cases. A method for calculating the internal force and stiffness of the stacked arch was proposed for better applications.

Compared to the stacked arch, the separated arch requires an additional drainage system. It is more complex to construct and less efficient to improve the stiffness and load-bearing capacity of the lining but is particularly suitable for strengthening and reinforcing the lining sections with water leakage problems [153]. Yu and Sang [149] used the 'load-structure method' to test the secondary lining structure with a single prefabricated longitudinal crack reinforced by the separated arch and analyzed the mechanical properties, damage modes, and ultimate bearing capacity of the reinforced lining structures. The results proved that the separated arch was very effective for tunnel retrofitting.

There are also many applications of the cover-arch reinforcement methods, such as the Bayi Tunnel in Chongqing [154], and the method could achieve better reinforcement and guarantee the stability of the tunnel operation. However, the process for the cover-arch method can be complicated and can seriously disrupt traffic. Additionally, the arch structure is typically made of concrete, which is thick and has a significant impact on the tunnel lining construction. Therefore, the range of applications of the cover-arch method is still restricted.

4.1.3 Bonded FRP method

Another popular method for reinforcing the inner surface of linings is the bonded FRP. FRP is characterized by high strength, durability, and ductility [155]. The mechanical properties and ductility of the damaged lining can be improved by pasting FRP to the lining with epoxy resin, and the lining will have greater load-carrying potential during the later stages of loading [156].

Many studies have been conducted to investigate the feasibility and effectiveness of FRP retrofitting. Wu and Cai [157] investigated the feasibility of fiber-reinforcing tunnels by monitoring the stability of the surrounding rock after reinforcing cracks in the tunnel lining. Ai et al. [158] used FRP to strengthen the tunnel lining and achieved their expected results, indicating that bonded FRP in the early deterioration stage could reduce retrofitting costs. Yang et al. [159] used the finite

element method to investigate the retrofitting effect of FRP reinforced cracked lining. The results revealed that when the FRP was bonded to the lining surface after the secondary lining cracked, the expansion of tensile cracks could be effectively avoided. Furthermore, Jiang et al. [160] proposed the so-called FRP-PCM method to strengthen degraded tunnel linings and simulated it numerically. The construction procedure of the FRP-PCM method was shown in **Fig. 38** [161]. The FRP-PCM method was based on strengthening tunnel linings by FRP grids, embedded in PCM (one of Polymer Cement Mortar). The study evaluated numerical models for various loosening pressures affecting the tunnel lining, taking into account factors such as the foundation grade, extent of lining degradation, and tunnel condition. Based on these evaluations, the study suggested appropriate conditions for implementing the FRP-PCM method to effectively reinforce the tunnel linings. However, it did not consider other unfavorable conditions beyond the loosening pressure. Han et al. [125] examined the reinforcement behavior of the FRP-PCM method on tunnel linings, and they observed that the plastic shear failure on the outer surface could be significantly suppressed and the long-term failure rate of the tunnel lining could also be significantly reduced. Additionally, previous studies all concentrated on enhancing the load-bearing capacity and stiffness of the lining through FRP reinforcement. However, its impact on the cracking behavior of the tunnel lining has not been explored yet. To address this, Liu et al. [162] examined the effect of FRP on controlling lining cracking under inclined pressure using scale tests. They analyzed the mechanism of its action and the influence of the number and arrangement of FRP grid layers on the reinforcement effect. The results demonstrate that as the amount of FRP increases, the ultimate load carrying capacity and structural stiffness of the tunnel lining increases significantly, while the ductility decreases.

Fig. 38. Application of the FRP-PCM method on tunnel linings: (a) surface treatment; (b) fix the FRP grids; (c) spay the PCM; (d) after the construction [161]**.**

Many researchers have also studied the factors that affect the effectiveness of the FRP retrofitting method. Li et al. [163] used numerical simulations to investigate the reinforcing effectiveness of using different lengths and layers of fiber cloth in terms of reinforcement forces and lining damage. Liu and Zhang [164] used numerical simulations to investigate the effect of FRP on tunnel lateral deformation, and they thoroughly analyzed the influence of ground resistance, bonded time, and the number of FRP layers on the retrofitting effectiveness. Liu et al. [165] investigated the use of FRP to strengthen longitudinal joints in shield tunnels and compared the structural performance and damage morphology of reinforced and unreinforced longitudinal joints. Their research revealed the damage mechanism of FRP-reinforced joints and made an overall evaluation of the efficiency of retrofitting. The results demonstrated that the bonded FRP could improve the corner stiffness of reinforced joints, but the bonded surface of FRP was the weak point of the entire structure. The retrofitting effect was determined by the bonded strength and shear strength of the structural adhesive materials. They also observed that FRP could only be used for the temporary strengthening of longitudinal joints, but not for long-term strengthening.

Compared to the bonded steel method and the cover-arch method, the bonded fiber method has a local reinforcement effect, with simple machinery and construction procedures [155]. However, the FRP fabric has higher requirements for the reinforcing and construction environment, as epoxy is vulnerable to high temperatures and moisture. The retrofitting effectiveness of bonded fiber

method is also affected by existing deformations, with larger deformations leading to weaker retrofitting effectiveness [166]. Moreover, due to the flexibility of the fiber, this retrofitting method is only suitable for the tensile zone, resulting in a local retrofitting effect that does not significantly improve the overall stiffness of the lining [167].

4.2 Grouting retrofitting

Previous research has shown that the pressure variation in the surrounding earth or rock is a major cause of damage to tunnel linings [168]. Therefore, in addition to the inner surface of the lining strengthening, it is also important to control the deformation of the lining by grouting the surrounding rock [169]. The reinforcing procedure of the tunnel grouting method is to inject the grouting slurry into the surrounding rock by producing holes, relying on the grouting pressure to spread the slurry into the fissures of the surrounding rock to form a reinforcement zone, as shown in **Fig. 39**. This improves the integrity and strength of the rock mass, which in turn reduces the lateral deformation of the tunnel, and solves the problems such as water leakage through the tunnel tubes, large differential settlement, and unstable tunnel deformations [170].

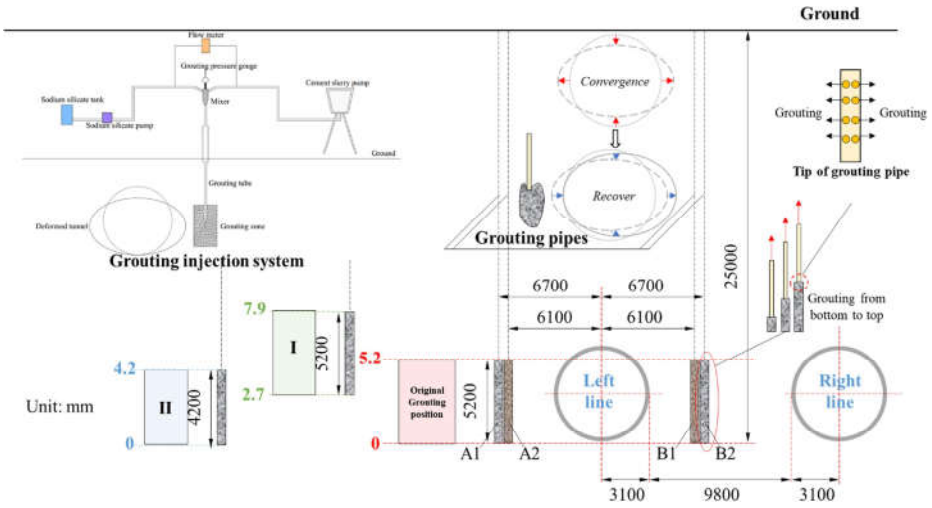

Fig. 39. The grouting system and working procedure [170].

Researchers have investigated the effectiveness of grouting reinforcement using various methods. The primary methods for investigating grouting retrofitting include field measurements and numerical simulations. The process is usually represented by simulating the volume expansion of predetermined elements that represent the grouted soil. The volume expansion can be achieved through two methods: (1) applying internal pressure or (2) applying volume strain directly to the

unit [171]. Soga et al. [172] described the internal pressure method using the 3D finite difference program FLAC3D. In this numerical procedure, target grids representing grout-treated zones and the total volumetric expansion rate $\Delta\varepsilon_v^t$ of these elements should be defined in advance. The parameter $\Delta\varepsilon_v^t$ serves as an indicator to judge the terminal of expansion:

$$\Delta\varepsilon_v^t = \frac{V_{inj}}{V_0} \tag{9}$$

where V_{inj} denotes the volume of grout injected into the soil, and V_0 denotes the initial volume of the same treated soil body. At the beginning of this procedure, the volumetric strain increment $\Delta\varepsilon_V$ of the target element is zero. In each iteration, a FISH program is used to modify the stress components $\sigma_i(i = x, y, z)$ of target elements by adding a small internal pressure p_i to each of them. The $\Delta\varepsilon_v^t$ increases as the calculation proceeds. In the volumetric strain method, a pre-determined strain is applied directly to the target elements. Based on the above theory, Xue et al. [173] tested the mechanical strength of the reinforced tunnel linings with cavities and weak surrounding rocks strengthened using the grouting method. The results demonstrated that the use of the slurry reinforcement led to a more uniform distribution of stress within the lining structure and the surrounding rock. A significant improvement in the overall stability of the lining structure was also achieved. Zhang et al. [169] used lateral convergence, joint opening, and grout-induced dislocation changes as indicators to analyze the impact of grouting on the lateral deformation of tunnels. The results demonstrated that grouting could successfully increase the lateral convergence of the tunnel and decrease the joint opening.

After determining the reinforcing effect of grouting, evaluating and improving its effectiveness is also an important issue. The horizontal convergence of the tunnel is one of the most commonly used performance indicators in practice for assessing the early effects of reinforcement [174–176]. When using grouting to control convergence in large tunnels, the parameters used are critical to the effectiveness of the treatment. These control parameters include the number of grouting rows, the construction sequence, and the horizontal distance between the grouting rows and the tunnel dimensions, as shown in **Fig. 40** [177]. To provide further confirmation of the relevant grouting parameters, Zhang et al. [177] conducted a case study to analyze the effect of grouting on reducing deformations in large tunnels. Recommendations for optimized grouting parameters were provided. However, the study did not discuss the long-term effect of grouting on convergence reduction due

to the lack of field data for validation. Future work will be focused on the long-term effects of grouting and the impact of soil swelling, in order to gain a deeper understanding of the effects of grouting.

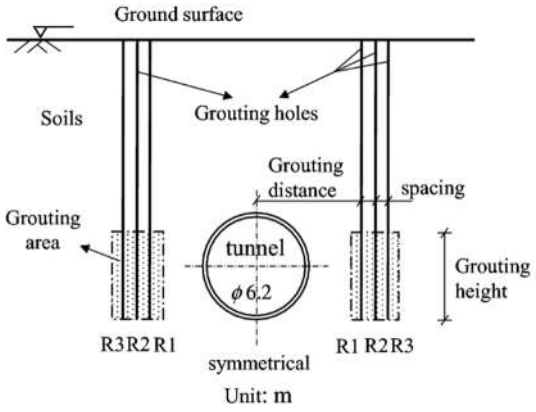

Fig. 40. Grouting parameters layout [177]**.**

Also, many grouting theories have been created, including the seepage grouting theory [178], the fracture grouting theory [179], and the compaction theory [180]. These theories reveal the variation law of grouting pressure, grout flow rate, diffusion radius, and grouting time in the grouting process and serve as guides for design and construction.

Some researchers have investigated the behavior of grouting materials. The two primary types of grouting used nowadays are cement slurry and chemical slurry. The inexpensive cement slurry provides excellent longevity, outstanding seepage resistance, and great strength after consolidation. However, due to inaccurate control issues and lack of strength, the utilization range of cement slurry is restricted [181]. The chemical slurry uses grouting materials such as polyurethane and epoxy resin with a regulated setting time and good permeability for a variety of applications, although they are more expensive [182,183].

Compared to the internal surface retrofitting methods, grouting can directly seal the fractures in the surrounding rock and fill the cavity to handle lining defects such as water leakage and cavities. It can also improve the resistance of the surrounding rocks. As the surrounding rock pressure increases, it can effectively reduce the deformation of the lining structure, which can furtherly avoid the development of other defects. However, determining the ideal grouting volume and pressure is difficult due to the complexity of the grouting retrofitting process and the numerous influencing factors. Inappropriate grouting procedures and techniques may be less effective and speed up the

progression of the defect [184].

4.3 Summary and outlook

In conclusion, a variety of retrofitting techniques have been developed, but these techniques and the reinforcing materials still need further investigation, as shown in **Table 8**. Previous studies on reinforcement technology only provide a limited summary of the reinforcement methods used for specific tunnel projects, lacking a comprehensive overview of the development of reinforcement technologies. Additionally, there is a lack of theoretical analysis, application statement, and comparison of these methods. With the above review, according to the latest developments and characteristics of the existing tunnel reinforcement methods, the authors believe that further research is needed in the following areas:

(1) Although the majority of current research focuses on one technology, the combination of different tunnel retrofitting techniques to achieve the overall performance of structures is worth investigating. Further investigation into the coupling mechanisms of various retrofitting technologies can be a good direction.

(2) The most common failure mode observed for internal surface retrofitting of tunnel linings is interfacial damage. However, the majority of current studies assume that the adhesion between the retrofitting material and the lining is sufficient, thus ignoring the interface damage and failing to reflect the fractural situation. Further research is required on the interface failure mechanism and anchorage control mechanisms for liner internal surface retrofitting.

(3) The design of lining retrofitting is still based on experience and there is a lack of quantitative design methods. Further exploration is needed to understand the mechanisms and develop corresponding design standards for various retrofitting methods.

Table 8 Comparison of different retrofitting methods

Retrofitting methods	Defects solved	Advantages	Disadvantages
Bonded steel plate [126–146]	Deformation Cracks	1) Short construction period; 2) Can address the overall strength and stiffness of the lining;	1) Higher cost; 2) Secondary damage to the lining; 3) Fragile bonding interface;

Cover-arch [147–154]	Deformation Cracks Leakage	The most effective method	1) Complex operation; 2) Long construction period; 3) Tunnel height restrictions;
Bonded FRP [125,155–167]	Deformation Cracks	1) Simple operation; 2) Short construction period;	1) Poor high-temperature resistance; 2) Difficult to use in the wet environment; 3) Only applicable to the tensile area;
Grouting [168–184]	Deformation Cracks Voids Leakage	Retrofitting of operating tunnels under micro disturbance	1) Complex operation; 2) May cause secondary damage to the tunnel;

5. Conclusions

To ensure the structural safety and extend the service life of the tunnel linings, it is necessary to conduct regular inspections on the structural health and maintenance of tunnels. Modern NDT methods can provide detailed information on tunnel lining defects. The suitability of these methods for representative defects (cracks, leakage, and voids) has been analyzed and summarized. Based on the qualitative or quantitative data, a summary of the procedures for the assessment of tunnel lining health states is also provided. Finally, different retrofitting techniques corresponding to various lining defects have also been reviewed. The following conclusions can be made:

(1) NDT methods should be selected based on specific requirements, such as fast mobile detection or accurate in-place measurement, and according to the characteristics of the targeted defect. For crack detection, vision-based methods combined with image processing or deep learning are commonly used to obtain the crack information on the surface, while the depth of the crack can be measured by the GPR or acoustic techniques. Leakage can be detected from visible light images, thermal infrared images, and laser intensity images. And radar or sonic/ultrasonic techniques are the most preferred methods of detecting voids behind tunnel linings. On the inspection of the internal state of the defects, tomography based on acoustic and electric mechanisms, among others, has proven to be a promising visualization method. For real-case applications with complex field conditions, it is recommended to use multiple sensing methods to conduct a comprehensive

inspection of tunnel defects. However, attention should also be paid to the contradictory points between different techniques, because they may have limitations in certain conditions or for certain types of defects. In addition, the inconsistent results of different methods may arise from different field conditions, detection resolution, data processing algorithms, measurement errors, and other factors. Therefore, a reasonable fusion strategy of different methods should be developed first to implement complementarity of them and provide accurate and comprehensive results. The future trend of tunnel lining inspection is towards more intelligent and automated systems that integrate multiple sensing techniques and NDT methods. In addition, there is a growing interest in the use of unmanned detection vehicles and robots to perform more complex and dangerous inspection tasks.

(2) Due to the demands of practical applications, the condition evaluation methods of tunnel linings are gradually transferring from qualitative to quantitative analysis. Generally, the methods can be divided into normative assessment method, mathematical model-based evaluation method, and artificial intelligence-based evaluation method. The normative assessment method is relatively comprehensive, although the accuracy of the evaluation results could be improved and manual intervention is usually inevitable. Mathematical model-based evaluation methods are accurate enough for a single indicator but cannot handle the correlation between different evaluation indicators. Artificial intelligence-based evaluation methods have great data processing capabilities and will provide good results if accurate and large databases are available before the evaluation. There is a trend to propose more effective indicators/models and combine the evaluation of tunnel linings with more advanced detection technologies. The condition evaluation of the tunnels will also become more comprehensive, accurate, and real-time.

(3) Retrofitting methods of tunnel lining defects can be divided into lining inner surface retrofitting and grouting retrofitting. The three main types of inner surface retrofitting methods are the bonded steel plate method, the cover-arch reinforcing, and the bonded FRP method. To improve the retrofitting effectiveness, the selected retrofitting methods should be based on the health condition, the mechanism of the defect, and the scope of application of the retrofitting method. To satisfy the increasing application demands, the next stage of research will focus on the physical mechanism, the coupling behaviors, and the design method of structural retrofitting.

Although after years of progress in these fields, there is still a gap between the performance of

the conventional methods and the application requirements of practical tunnels. There are still some challenges to overcome in the future. More research is needed, especially on the development of integrated and intelligent inspection systems, comprehensive tunnel condition evaluation methods, and effective proven reinforcement techniques with clearer mechanisms. Meanwhile, efforts are also needed to establish effective cooperation mechanisms between detection, evaluation and retrofitting, and finally to develop a comprehensive health monitoring and maintenance system for tunnel linings.

This paper is an up-to-date and comprehensive review that covers the entire framework of tunnel lining detection and retrofitting, which has not been conducted before. It can provide systematic guidance and useful reference for understanding the state of the art of tunnel inspection, health evaluation, and retrofitting methods.

Acknowledgement

The authors would like to thank the financial supports from the National Natural Science Foundation of China (NSFC) (Grant Number: 52208215), the Natural Science Foundation of Zhejiang Province (Grant Number: LQ22E080008) and The Center for Balance Architecture of Zhejiang University.

Author Contribution Statement

Yandan Jiang: Writing – review & editing, Writing – original draft, Supervision. Lai Wang: Writing – review & editing, Methodology, Investigation. Bo Zhang: Writing – review & editing, Investigation. Xiaowei Dai: Writing – review & editing, Investigation. Bochao Sun: Writing – review & editing, Investigation. Nianwu Liu: Writing – review & editing. Zhen Wang: Writing – review & editing. Jun Ye: Writing – review & editing, Supervision, Resources, Project Administration, Funding Acquisition, Conceptualization. Yang Zhao: Writing – review & editing, Resources, Project Administration, Funding Acquisition

References

[1] H.M. Lyu, S.L. Shen, A. Zhou, Z.Y. Yin, Assessment of safety status of shield tunnelling using operational parameters with enhanced SPA, Tunnelling and Underground Space Technology. 123 (2022) 104428. https://doi.org/10.1016/j.tust.2022.104428.

[2] D. Liu, F. Zhong, H. Huang, J. Zuo, Y. Xue, D. Zhang, Present status and development trend of diagnosis and treatment of tunnel lining diseases, China Journal of Highway and Transport. 34 (11) (2021), pp. 178–199 (in Chinese). https://doi.org/10.19721/j.cnki.1001-7372.2021.11.015.

[3] D. Zhao, X. Tan, L. Jia, Study on investigation and analysis of existing railway tunnel diseases, Applied Mechanics and Materials. 580–583 (2014), pp. 1218–1222. https://doi.org/10.4028/www.scientific.net/AMM.580-583.1218.

[4] H. Huang, L. Chen, Risk analysis of building structure due to shield tunneling in urban area, Underground Construction and Ground Movement. (2006), pp. 150–157. https://doi.org/10.1061/40867(199)17.

[5] ITA-AITES, Tunnel Market Survey 2019. https://mtry.fi/tunnel-market-survey-2019-ita-aites (Last accessed in February 17th, 2023).

[6] Y. Zhao, P. Li, A statistical analysis of China's traffic tunnel development data, Engineering. 4 (1) (2018), pp. 3–5. https://doi.org/10.1016/j.eng.2017.12.011.

[7] H. Mashimo, T. Ishimura, State of the art and future prospect of maintenance and operation of road tunnel, in: ISARC. Proceedings of the 23rd International Symposium on Automation and Robotics in Construction, IAARC Publications, 2006, pp. 299–302. https://doi.org/10.22260/isarc2006/0057 (ISBN 9784990271718).

[8] W. Liu, X. Wu, L. Zhang, Y. Wang, J. Teng, Sensitivity analysis of structural health risk in operational tunnels, Automation in Construction. 94 (2018), pp. 135–153. https://doi.org/10.1016/j.autcon.2018.06.008.

[9] Z. Huang, H. Fu, W. Chen, J. Zhang, H. Huang, Damage detection and quantitative analysis of shield tunnel structure, Automation in Construction. 94 (2018), pp. 303–316. https://doi.org/10.1016/j.autcon.2018.07.006.

[10] L. Attard, C.J. Debono, G. Valentino, M. Di Castro, Tunnel inspection using photogrammetric techniques and image processing: A review, ISPRS Journal of Photogrammetry and Remote Sensing. 144 (2018), pp. 180–188. https://doi.org/10.1016/j.isprsjprs.2018.07.010.

[11] Q. Ai, Y. Yuan, S.L. Shen, H. Wang, X. Huang, Investigation on inspection scheduling for the maintenance of tunnel with different degradation modes, Tunnelling and Underground Space Technology. 106 (2020) 103589. https://doi.org/10.1016/j.tust.2020.103589.

[12] K. Elbaz, J.S. Shen, A. Arulrajah, S. Horpibulsuk, Geohazards induced by anthropic activities of geoconstruction: a review of recent failure cases, Arabian Journal of Geosciences. 9 (18) (2016), pp. 1–11. https://doi.org/10.1007/s12517-016-2740-z.

[13] C. Liu, D. Zhang, S. Zhang, Characteristics and treatment measures of lining damage: A case study on a mountain tunnel, Engineering Failure Analysis. 128 (2021) 105595. https://doi.org/10.1016/j.engfailanal.2021.105595.

[14] W. Bergeson, S.L. Ernst, Tunnel Operations, Maintenance, Inspection, and Evaluation (TOMIE) Manual, United States. Federal Highway Administration (2015), FHWA-HIF-15-

005. https://rosap.ntl.bts.gov/view/dot/42887 (Last accessed in December 2nd, 2022).
[15] J.M.W. Brownjohn, Structural health monitoring of civil infrastructure, Philosophical Transactions of the Royal Society A: Mathematical, Physical and Engineering Sciences. 365 (1851) (2007), pp. 589–622. https://doi.org/10.1098/rsta.2006.1925.
[16] D. Feng, M.Q. Feng, Computer vision for SHM of civil infrastructure: From dynamic response measurement to damage detection–A review, Engineering Structures. 156 (2018), pp. 105–117. https://doi.org/10.1016/j.engstruct.2017.11.018.
[17] C. Balaguer, R. Montero, J.G. Victores, S. Martínez, A. Jardón, Towards fully automated tunnel inspection: A survey and future trends, in: ISARC. Proceedings of the 31st International Symposium on Automation and Robotics in Construction, IAARC Publications, 2014, pp. 19–33. https://doi.org/10.22260/isarc2014/0005 (ISBN 978-0-646-59711-9).
[18] Y.A. Hsieh, Y.J. Tsai, Machine learning for crack detection: Review and model performance comparison, Journal of Computing in Civil Engineering. 34 (5) (2020) 04020038. https://doi.org/10.1061/(ASCE)CP.1943-5487.0000918.
[19] C. Koch, K. Georgieva, V. Kasireddy, B. Akinci, P. Fieguth, A review on computer vision based defect detection and condition assessment of concrete and asphalt civil infrastructure, Advanced Engineering Informatics. 29 (2) (2015), pp. 196–210. https://doi.org/10.1016/j.aei.2015.01.008.
[20] E. Menendez, J.G. Victores, R. Montero, S. Martínez, C. Balaguer, Tunnel structural inspection and assessment using an autonomous robotic system, Automation in Construction. 87 (2018), pp. 117–126. https://doi.org/10.1016/j.autcon.2017.12.001.
[21] D.M. McCann, M.C. Forde, Review of NDT methods in the assessment of concrete and masonry structures, NDT & E International. 34 (2) (2001), pp. 71–84. https://doi.org/10.1016/S0963-8695(00)00032-3.
[22] W.W.L. Lai, X. Dérobert, P. Annan, A review of Ground Penetrating Radar application in civil engineering: A 30-year journey from Locating and Testing to Imaging and Diagnosis, NDT & E International. 96 (2018), pp. 58–78. https://doi.org/10.1016/j.ndteint.2017.04.002.
[23] K. Schabowicz, Modern acoustic techniques for testing concrete structures accessible from one side only, Archives of Civil and Mechanical Engineering. 15 (4) (2015), pp. 1149–1159. https://doi.org/10.1016/j.acme.2014.10.001.
[24] R. Montero, J.G. Victores, S. Martínez, A. Jardón, C. Balaguer, Past, present and future of robotic tunnel inspection, Automation in Construction. 59 (2015), pp. 99–112. https://doi.org/10.1016/j.autcon.2015.02.003.
[25] Y. Jiang, X. Zhang, T. Taniguchi, Quantitative condition inspection and assessment of tunnel lining, Automation in Construction. 102 (2019), pp. 258–269. https://doi.org/10.1016/j.autcon.2019.03.001.
[26] X. Li, X. Lin, H. Zhu, X. Wang, Z. Liu, Condition assessment of shield tunnel using a new indicator: The tunnel serviceability index, Tunnelling and Underground Space Technology. 67 (2017), pp. 98–106. https://doi.org/10.1016/j.tust.2017.05.007.
[27] M. Alsharqawi, T. Dawood, S. Abdelkhalek, M. Abouhamad, T. Zayed, Condition assessment of concrete-made structures using ground penetrating radar, Automation in Construction. 144 (2022) 104627. https://doi.org/10.1016/j.autcon.2022.104627.
[28] J. Lai, J. Qiu, H. Fan, J. Chen, Z. Hu, Q. Zhang, J. Wang, Structural safety assessment of existing multiarch tunnel: a case study, Advances in Materials Science and Engineering.

2017 (2017). https://doi.org/10.1155/2017/1697041.
[29] X. Wu, Y. Jiang, J. Wang, K. Masaya, T. Taniguchi, T. Yamato, A new health assessment index of tunnel lining based on the digital inspection of surface cracks, Applied Sciences. 7 (5) (2017) 507. https://doi.org/10.3390/app7050507.
[30] M. Zhu, H. Zhu, F. Guo, X. Chen, J.W. Ju, Tunnel condition assessment via cloud model-based random forests and self-training approach, Computer-Aided Civil and Infrastructure Engineering. 36 (2) (2021), pp. 164–179. https://doi.org/10.1111/mice.12601.
[31] T. Asakura, Y. Kojima, Tunnel maintenance in Japan, Tunnelling and Underground Space Technology. 18 (2-3) (2003), pp. 161–169. https://doi.org/10.1016/S0886-7798(03)00024-5.
[32] J.A. Richards, Inspection, maintenance and repair of tunnels: international lessons and practice, Tunnelling and Underground Space Technology. 13 (4) (1998), pp. 369–375. https://doi.org/10.1016/s0886-7798(98)00079-0.
[33] F. Ye, N. Qin, X. Liang, A. Ouyang, Z. Qin, E. Su, Analyses of the defects in highway tunnels in China, Tunnelling and Underground Space Technology. 107 (2021) 103658. https://doi.org/10.1016/j.tust.2020.103658.
[34] L.R. Sousa, R.L. Sousa, C. Silva, V. Freitas, Maintenance methodologies of old railway tunnels, in: Symposium New Development in Rock Mechanics and Engineering & Sanya Forum for the Plan of City and City Construction, 2009, pp. 401–406. https://www.researchgate.net/profile/Luis-Sousa-3/publication/271763635_Maintenance_methodologies_of_old_railway_tunnels (Last accessed in March 12th, 2023).
[35] T. Rock, P. Arch, T. Ireland, Rehabilitation and maintenance of road tunnels–Mersey Queensway, in: IABSE Symposium Report, International Association for Bridge and Structural Engineering, 2006, pp. 33–40. https://doi.org/10.2749/222137806796235953.
[36] T. Liu, H. Zhu, Research on defects of arcade tunnel with partial pressure and its treating measurements, China Journal of Highway and Transport. 18 (4) (2005), pp. 72–77 (in Chinese). https://doi.org/10.19721/j.cnki.1001-7372.2005.04.015.
[37] Y. Luo, J. Chen, Research status and progress of tunnel frost damage, Journal of Traffic and Transportation Engineering (English Edition). 6 (3) (2019), pp. 297–309. https://doi.org/10.1016/j.jtte.2018.09.007.
[38] H. Feng, X. Zhang, D. Gou, J. Chun, X. Ou, X. Zhou, Cause investigation of side-wall cracking in an operational tunnel, Engineering Failure Analysis. 101 (2019), pp. 157–171. https://doi.org/10.1016/j.engfailanal.2019.02.038.
[39] F. Ye, X. Han, N. Qin, A. Ouyang, X. Liang, C. Xu, Damage management and safety evaluation for operating highway tunnels: a case study of Liupanshan tunnel, Structure and Infrastructure Engineering. 16 (11) (2020), pp. 1512–1523. https://doi.org/10.1080/15732479.2020.1713165.
[40] X. Zhang, Y. Jiang, K. Maegawa, Mountain tunnel under earthquake force: A review of possible causes of damages and restoration methods, Journal of Rock Mechanics and Geotechnical Engineering. 12 (2) (2020), pp. 414–426. https://doi.org/10.1016/j.jrmge.2019.11.002.
[41] H. Feng, X. Chang, Analysis of structural disasters in shield tunnels and measures and suggestions for waterproofing, Modern Tunnelling Technology. 53 (6) (2016), pp. 36–43 (in Chinese). https://doi.org/10.13807/j.cnki.mtt.2016.06.006.

[42] F. Dong, Q. Fang, D. Zhang, H. Xu, Y. Li, X. Niu, Analysis on defects of operational metro tunnels in Beijing, China Civil Engineering Journal. 50 (6) (2017), pp. 104–113 (in Chinese). https://doi.org/10.15951/j.tmgcxb.2017.06.012.
[43] A. Inokuma, S. Inano, Road tunnels in Japan: deterioration and countermeasures, Tunnelling and Underground Space Technology. 11 (3) (1996), pp. 305–309. https://doi.org/10.1016/0886-7798(96)00026-0.
[44] S.W. Park, Y.S. Shin, Y.S. Oh, S.R. Ahn, A guideline on condition assessment of existing old railway tunnels, Tunnelling and Underground Space Technology. 21 (3-4) (2006), pp. 329–330. https://doi.org/10.1016/j.tust.2005.12.043.
[45] C. Yuan, S. Li, S. Li, W. Li, Study of defects characteristics and repair methods of old tunnel in cold region, Chinese Journal of Rock Mechanics and Engineering. 30 (S1) (2011), pp. 3354–3361 (in Chinese). https://kns.cnki.net/kcms/detail/detail.aspx?FileName=YSLX2011S1099&DbName=CJFQ2011 (Last accessed in March 12th, 2023).
[46] S. Zhao, M. Shadabfar, D. Zhang, J. Chen, H. Huang, Deep learning-based classification and instance segmentation of leakage-area and scaling images of shield tunnel linings, Structural Control and Health Monitoring. 28 (6) (2021) e2732. https://doi.org/10.1002/stc.2732.
[47] Q. Gong, L. Zhu, Y. Wang, Z. Yu, Automatic subway tunnel crack detection system based on line scan camera, Structural Control and Health Monitoring. 28 (8) (2021) e2776. https://doi.org/10.1002/stc.2776.
[48] M. Lei, L. Liu, C. Shi, Y. Tan, Y. Lin, W. Wang, A novel tunnel-lining crack recognition system based on digital image technology, Tunnelling and Underground Space Technology. 108 (2021) 103724. https://doi.org/10.1016/j.tust.2020.103724.
[49] Q. Wang, N. Zhang, K. Jiang, C. Ma, Z. Zhou, C. Dai, Tunnel lining crack recognition based on improved multiscale retinex and sobel edge detection, Mathematical Problems in Engineering. 2021 (2021). https://doi.org/10.1155/2021/9969464.
[50] T. Yu, A. Zhu, Y. Chen, Efficient crack detection method for tunnel lining surface cracks based on infrared images, Journal of Computing in Civil Engineering. 31 (3) (2017) 04016067. https://doi.org/10.1061/(asce)cp.1943-5487.0000645.
[51] Y. Xue, Y. Li, A fast detection method via region-based fully convolutional neural networks for shield tunnel lining defects, Computer-Aided Civil and Infrastructure Engineering. 33 (8) (2018), pp. 638–654. https://doi.org/10.1111/mice.12367.
[52] Y. Ren, J. Huang, Z. Hong, W. Lu, J. Yin, L. Zou, X. Shen, Image-based concrete crack detection in tunnels using deep fully convolutional networks, Construction and Building Materials. 234 (2020) 117367. https://doi.org/10.1016/j.conbuildmat.2019.117367.
[53] X. Xu, H. Yang, Vision measurement of tunnel structures with robust modelling and deep learning algorithms, Sensors. 20 (17) (2020) 4945. https://doi.org/10.3390/s20174945.
[54] S. Zhao, D. Zhang, Y. Xue, M. Zhou, H. Huang, A deep learning-based approach for refined crack evaluation from shield tunnel lining images, Automation in Construction. 132 (2021) 103934. https://doi.org/10.1016/j.autcon.2021.103934.
[55] D. Li, Q. Xie, X. Gong, Z. Yu, J. Xu, Y. Sun, J. Wang, Automatic defect detection of metro tunnel surfaces using a vision-based inspection system, Advanced Engineering Informatics. 47 (2021) 101206. https://doi.org/10.1016/j.aei.2020.101206.
[56] A.P. Annan, GPR — History, trends, and future developments, Subsurface Sensing

Technologies and Applications. 3 (4) (2002), pp. 253–270. https://doi.org/10.1023/A:1020657129590.
[57] G. Alsharahi, M.F. Bouami, A. Faize, M. Louzazni, A. Khamlichi, M. Atounti, Contribution of analysis and detection the risks appearing in roads using GPR method: A case study in Morocco, Ain Shams Engineering Journal. 12 (2) (2021), pp. 1435–1450. https://doi.org/10.1016/j.asej.2020.10.014.
[58] L. Xiang, H. Zhou, Z. Shu, S. Tan, G. Liang, J. Zhu, GPR evaluation of the Damaoshan highway tunnel: A case study, NDT & E International. 59 (2013), pp. 68–76. https://doi.org/10.1016/j.ndteint.2013.05.004.
[59] D. Feng, X. Wang, B. Zhang, Specific evaluation of tunnel lining multi-defects by all-refined GPR simulation method using hybrid algorithm of FETD and FDTD, Construction and Building Materials. 185 (2018), pp. 220–229. https://doi.org/10.1016/j.conbuildmat.2018.07.039.
[60] D. Liu, Y. Deng, F. Yang, G. Xu, Nondestructive testing for crack of tunnel lining using GPR, Journal of Central South University of Technology. 12 (1) (2005), pp. 120–124. https://doi.org/10.1007/s11771-005-0384-3.
[61] T. Ling, L. Zhang, F. Huang, D. Gu, B. Yu, S. Zhang, OMHT method for weak signal processing of GPR and its application in identification of concrete micro-crack, Journal of Central South University. 26 (11) (2019), pp. 3057–3065. https://doi.org/10.1007/s11771-019-4236-y.
[62] M. Moles, L. Robertson, T. Sinclair, Developments in time-of-flight diffraction (TOFD), in: 18th World Conference on Nondestructive Testing, 2012. https://www.ndt.net/search/docs.php3?id=12563 (Last accessed in March 14th, 2023).
[63] M. Spies, H. Rieder, A. Dillhöfer, V. Schmitz, W. Müller, Synthetic aperture focusing and time-of-flight diffraction ultrasonic imaging—past and present, Journal of Nondestructive Evaluation. 31 (4) (2012), pp. 310–323. https://doi.org/10.1007/s10921-012-0150-z.
[64] A. Habibpour-Ledari, F. Honarvar, Three dimensional characterization of defects by ultrasonic time-of-flight diffraction (ToFD) technique, Journal of Nondestructive Evaluation. 37 (1) (2018), pp. 1–11. https://doi.org/10.1007/s10921-018-0465-5.
[65] Y.C. Angel, J.D. Achenbach, Reflection and transmission of obliquely incident Rayleigh waves by a surface-breaking crack, The Journal of the Acoustical Society of America. 75 (2) (1984), pp. 313–319. https://doi.org/10.1121/1.390473.
[66] C.H. Yew, K.G. Chen, D.L. Wang, An experimental study of interaction between surface waves and a surface breaking crack, The Journal of the Acoustical Society of America. 75 (1) (1984), pp. 189–196. https://doi.org/10.1121/1.390393.
[67] S.H. Kee, E. Fernández-Gómez, J. Zhu, Evaluating surface-breaking cracks in concrete using air-coupled sensors, ACI Materials Journal. 108 (5) (2011), pp. 558–565. https://doi.org/10.14359/51683266.
[68] S.H. Kee, J. Zhu, Using air-coupled sensors to determine the depth of a surface-breaking crack in concrete, The Journal of the Acoustical Society of America. 127 (3) (2010), pp. 1279–1287. https://doi.org/10.1121/1.3298431.
[69] C.W. In, F. Schempp, J.Y. Kim, L.J. Jacobs, A fully non-contact, air-coupled ultrasonic measurement of surface breaking cracks in concrete, Journal of Nondestructive Evaluation. 34 (1) (2015), pp. 1–7. https://doi.org/10.1007/s10921-014-0272-6.

[70] K. Karhunen, A. Seppänen, A. Lehikoinen, P.J.M. Monteiro, J.P. Kaipio, Electrical resistance tomography imaging of concrete, Cement and Concrete Research. 40 (1) (2010), pp. 137–145. https://doi.org/10.1016/j.cemconres.2009.08.023.
[71] K. Karhunen, A. Seppänen, A. Lehikoinen, J. Blunt, J.P. Kaipio, P.J.M. Monteiro, Electrical resistance tomography for assessment of cracks in concrete, ACI Materials Journal. 107 (5) (2010), pp. 523–531. https://doi.org/10.14359/51663973.
[72] T. Yasuda, H. Yamamoto, M. Enomoto, Y. Nitta, Smart tunnel inspection and assessment using mobile inspection vehicle, non-contact radar and AI, in: ISARC. Proceedings of the 37th International Symposium on Automation and Robotics in Construction, IAARC Publications, 2020, pp. 1373–1379. https://doi.org/10.22260/isarc2020/0190 (ISBN 978-952-94-3634-7).
[73] H. Huang, Y. Sun, Y. Xue, F. Wang, Inspection equipment study for subway tunnel defects by grey-scale image processing, Advanced Engineering Informatics. 32 (2017), pp. 188–201. https://doi.org/10.1016/j.aei.2017.03.003.
[74] N. Otsu, A threshold selection method from gray-level histograms, IEEE Transactions on Systems, Man, and Cybernetics. 9 (1) (1979), pp. 62–66. https://doi.org/10.1109/tsmc.1979.4310076.
[75] H. Huang, Q. Li, D. Zhang, Deep learning based image recognition for crack and leakage defects of metro shield tunnel, Tunnelling and Underground Space Technology. 77 (2018), pp. 166–176. https://doi.org/10.1016/j.tust.2018.04.002.
[76] Y. Xue, X. Cai, M. Shadabfar, H. Shao, S. Zhang, Deep learning-based automatic recognition of water leakage area in shield tunnel lining, Tunnelling and Underground Space Technology. 104 (2020) 103524. https://doi.org/10.1016/j.tust.2020.103524.
[77] D. Meng, S. Lin, H. Azari, Reducing thermal reflections for infrared thermography applications on tunnel liners with reflective finishes, Transportation Research Record. 2672 (41) (2018), pp. 145–155. https://doi.org/10.1177/0361198118780711.
[78] P. Yu, H. Wu, C. Liu, Z. Xu, Water leakage diagnosis in metro tunnels by intergration of laser point cloud and infrared thermal imaging, ISPRS-International Archives of the Photogrammetry, Remote Sensing and Spatial Information Sciences. 42 (2018), pp. 2167–2171. https://doi.org/10.5194/isprs-archives-xlii-3-2167-2018.
[79] Z. Lu, F. Zhu, L. Shi, F. Wang, P. Zeng, J. Hu, X. Liu, Y. Xu, Q. Chen, Automatic seepage detection in cable tunnels using infrared thermography, Measurement Science and Technology. 30 (11) (2019) 115902. https://doi.org/10.1088/1361-6501/ab30d9.
[80] H. Huang, W. Cheng, M. Zhou, J. Chen, S. Zhao, Towards automated 3D inspection of water leakages in shield tunnel linings using mobile laser scanning data, Sensors. 20 (22) (2020) 6669. https://doi.org/10.3390/s20226669.
[81] T. Xu, L. Xu, X. Li, J. Yao, Detection of water leakage in underground tunnels using corrected intensity data and 3D point cloud of terrestrial laser scanning, IEEE Access. 6 (2018), pp. 32471–32480. https://doi.org/10.1109/access.2018.2842797.
[82] X. Cheng, X. Hu, K. Tan, L. Wang, L. Yang, Automatic detection of shield tunnel leakages based on terrestrial mobile LiDAR intensity images using deep learning, IEEE Access. 9 (2021), pp. 55300–55310. https://doi.org/10.1109/ACCESS.2021.3070813.
[83] C. Lin, X. Wang, Y. Li, F. Zhang, Z. Xu, Y. Du, Forward modelling and GPR imaging in leakage detection and grouting evaluation in tunnel lining, KSCE Journal of Civil

Engineering. 24 (2020), pp. 278–294. https://doi.org/10.1007/s12205-020-1530-z.
[84] A. Voss, M. Pour-Ghaz, M. Vauhkonen, A. Seppänen, Electrical capacitance tomography to monitor unsaturated moisture ingress in cement-based materials, Cement and Concrete Research. 89 (2016), pp. 158–167. https://doi.org/10.1016/j.cemconres.2016.07.011.
[85] Y. Lyu, H. Wang, J. Gong, GPR detection of tunnel lining cavities and reverse-time migration imaging, Applied Geophysics. 17 (1) (2020), pp. 1–7. https://doi.org/10.1007/s11770-019-0831-9.
[86] A.M. Alani, F. Tosti, GPR applications in structural detailing of a major tunnel using different frequency antenna systems, Construction and Building Materials. 158 (2018), pp. 1111–1122. https://doi.org/10.1016/j.conbuildmat.2017.09.100.
[87] Q. Yu, H. Zhou, Y. Wang, R. Duan, Quality monitoring of metro grouting behind segment using ground penetrating radar, Construction and Building Materials. 110 (2016), pp. 189–200. https://doi.org/10.1016/j.conbuildmat.2015.12.109.
[88] H. Qin, D. Zhang, Y. Tang, Y. Wang, Automatic recognition of tunnel lining elements from GPR images using deep convolutional networks with data augmentation, Automation in Construction. 130 (2021) 103830. https://doi.org/10.1016/j.autcon.2021.103830.
[89] B. Liu, Y. Ren, H. Liu, H. Xu, Z. Wang, A.G. Cohn, P. Jiang, GPRInvNet: Deep learning-based ground-penetrating radar data inversion for tunnel linings, IEEE Transactions on Geoscience and Remote Sensing. 59 (10) (2021), pp. 8305–8325. https://doi.org/10.1109/TGRS.2020.3046454.
[90] Y. Zan, Z. Li, G. Su, X. Zhang, An innovative vehicle-mounted GPR technique for fast and efficient monitoring of tunnel lining structural conditions, Case Studies in Nondestructive Testing and Evaluation. 6 (2016), pp. 63–69. https://doi.org/10.1016/j.csndt.2016.10.001.
[91] Z. Ye, Y. Ye, Comparison of detection effect of cavities behind shield tunnel segment using transient electromagnetic radar and ground penetration radar, Geotechnical and Geological Engineering. 37 (5) (2019), pp. 4391–4403. https://doi.org/10.1007/s10706-019-00916-y.
[92] Z. Ye, C. Zhang, Y. Ye, Principle of a low-frequency transient electromagnetic radar system and its application in the detection of underground pipelines and voids, Tunnelling and Underground Space Technology. 122 (2022) 104392. https://doi.org/10.1016/j.tust.2022.104392.
[93] N.J. Carino, The impact-echo method: an overview, in: Structures 2001: A Structural Engineering Odyssey. (2001), pp. 1–18. https://doi.org/10.1061/40558(2001)15 (ISBN 9780784405581).
[94] R. Cao, M. Ma, R. Liang, C. Niu, Detecting the void behind the tunnel lining by impact-echo methods with different signal analysis approaches, Applied Sciences. 9 (16) (2019) 3280. https://doi.org/10.3390/app9163280.
[95] K. Hashimoto, T. Shiotani, T. Nishida, T. Miyagawa, Application of elastic-wave tomography to repair inspection in deteriorated concrete structures, Journal of Disaster Research. 12 (3) (2017), pp. 496–505. https://doi.org/10.20965/jdr.2017.p0496.
[96] H. Wang, S.H. Hsieh, C.H. Hu, Y.C. Tsai, Tracing developing deterioration zones in a damaged dam by using elastic wave tomography, in: IOP Conference Series: Materials Science and Engineering, IOP Publishing. 615 (1) (2019) 012077. https://doi.org/10.1088/1757-899x/615/1/012077.
[97] J. White, Ultrasonic tomography for detecting and locating defects in concrete structures,

PhD Thesis, Texas A & M University, 2012. https://core.ac.uk/download/pdf/147229609.pdf (Last accessed in March 12th, 2023).
[98] C.W. Tseng, Y.F. Chang, C.Y. Wang, Total focusing method or phased array technique: Which detection technique is better for the ultrasonic nondestructive testing of concrete?, Journal of Materials in Civil Engineering. 30 (1) (2018) 04017256. https://doi.org/10.1061/(ASCE)MT.1943-5533.0002118.
[99] S. Konishi, K. Kawakami, M. Taguchi, Inspection method with infrared thermometry for detect void in subway tunnel lining, Procedia Engineering. 165 (2016), pp. 474–483. https://doi.org/10.1016/j.proeng.2016.11.723.
[100] A. Afshani, K. Kawakami, S. Konishi, H. Akagi, Study of infrared thermal application for detecting defects within tunnel lining, Tunnelling and Underground Space Technology. 86 (2019), pp. 186–197. https://doi.org/10.1016/j.tust.2019.01.013.
[101] P. Cotič, D. Kolarič, V.B. Bosiljkov, V. Bosiljkov, Z. Jagličić, Determination of the applicability and limits of void and delamination detection in concrete structures using infrared thermography, NDT & E International. 74 (2015), pp. 87–93. https://doi.org/10.1016/j.ndteint.2015.05.003.
[102] S. Cui, J.K. Nimmagadda, J.E. Baciak, Backscatter radiography as a non-destructive examination tool for concrete structures, in: 2017 IEEE Nuclear Science Symposium and Medical Imaging Conference (NSS/MIC), IEEE, 2017, pp. 1–6. https://doi.org/10.1109/nssmic.2017.8532696.
[103] Y.D. Ye, H.H. Zhu, R.L. Wang, Analysis on the current status of metro operating tunnel damage in soft ground and its causes, Chinese Journal of Underground Space and Engineering. 3 (1) (2007), pp. 157–160 (in Chinese). https://doi.org/10.3969/j.issn.1673-0836.2007.01.034.
[104] P. Shi, P. Li, Mechanism of soft ground tunnel defect generation and functional degradation, Tunnelling and Underground Space Technology. 50 (2015), pp. 334–344. https://doi.org/10.1016/j.tust.2015.08.002.
[105] Highway and rail transit tunnel inspection manual, Federal Highway Administration and Federal Transit Administration, 2005. https://rosap.ntl.bts.gov/view/dot/40562 (Last accessed in February 17th, 2023).
[106] X.T. Lin, X.S. Chen, D. Su, M. Zhu, K.H. Han, R.P. Chen, Evaluation method for resilience of shield tunnel lining considering multiple disturbances and its application, Chinese Journal of Geotechnical Engineering. 44 (4) (2022), pp. 591–601 (in Chinese). http://f6z.cn/8iAoD (Last accessed in March 15th, 2023).
[107] Technical Specifications of Maintenance for Highway Tunnel JTGH12-2015, Ministry of Construction of the People's Republic of China, 2015 (in Chinese). https://www.nssi.org.cn/nssi/front/87846803.html (Last accessed in March 12th, 2023).
[108] Code for Design of Metro GB50157-2003, Ministry of Construction of the People's Republic of China, 2003 (in Chinese). https://www.nssi.org.cn/nssi/front/6257453.html (Last accessed in March 12th, 2023).
[109] Standard for Design of Shield Tunnel Engineering GB/T51438-2021, Ministry of Construction of the People's Republic of China, 2021 (in Chinese). https://www.nssi.org.cn/nssi/front/115026850.html (Last accessed in March 12th, 2023).
[110] Y. Shigeta, T. Tobita, K. Kamemura, M. Shinji, I. Yoshitake, K. Nakagawa, Propose of tunnel

crack index (TCI) as an evaluation method for lining concrete, Doboku Gakkai Ronbunshuu. 62 (4) (2006), pp. 628–632 (in Japanese). https://doi.org/10.2208/jscejf.62.628.
[111] B. Yu, J. Zhao, K. Fang, Y. Tan, J. Ning, Rock strength evaluation during progressive failure process based on fractural characterization, Marine Georesources & Geotechnology. 34 (8) (2016), pp. 759–763. https://doi.org/10.1080/1064119X.2015.1089454.
[112] W. Tian, N. Han, Evaluation of damage in concrete suffered freeze-thaw cycles by CT technique, Journal of Advanced Concrete Technology. 14 (11) (2016), pp. 679–690. https://doi.org/10.3151/jact.14.679.
[113] Y. Yuan, Y. Bai, J. Liu, Assessment service state of tunnel structure, Tunnelling and Underground Space Technology. 27 (1) (2012), pp. 72–85. https://doi.org/10.1016/j.tust.2011.07.002.
[114] X. Lin, W. Ding, X. Li, Y. Xi, Q. Yuan, GIS-Based grid assessment model of shield tunnel conditions and its application, Modern Tunnelling Technology. 55 (5) (2018), pp. 19–26 (in Chinese). https://doi.org/10.13807/j.cnki.mtt.2018.05.003.
[115] G. Andreotti, G.M. Calvi, K. Soga, C. Gong, W. Ding, Cyclic model with damage assessment of longitudinal joints in segmental tunnel linings, Tunnelling and Underground Space Technology. 103 (2020) 103472. https://doi.org/10.1016/j.tust.2020.103472.
[116] H. Zhang, X. Wang, Y. Xue, J. Zhu, Service status evaluation of shield tunnel based on Knowledge Graph, Modern Tunnelling Technology. 59 (4) (2022), pp. 58–68 (in Chinese). https://doi.org/10.13807/j.cnki.mtt.2022.04.007.
[117] M.H. Rafiei, H. Adeli, A novel unsupervised deep learning model for global and local health condition assessment of structures, Engineering Structures. 156 (2018), pp. 598–607. https://doi.org/10.1016/j.engstruct.2017.10.070.
[118] S.N. Yu, J.H. Jang, C.S. Han, Auto inspection system using a mobile robot for detecting concrete cracks in a tunnel, Automation in Construction. 16 (3) (2007), pp. 255–261. https://doi.org/10.1016/j.autcon.2006.05.003.
[119] J.G. Victores, S. Martínez, A. Jardón, C. Balaguer, Robot-aided tunnel inspection and maintenance system by vision and proximity sensor integration, Automation in Construction. 20 (5) (2011), pp. 629–636. https://doi.org/10.1016/j.autcon.2010.12.005.
[120] X. Chen, G. Liu, Z. Chen, Y. Li, C. Luo, B. Luo, X. Zhang, Automatic detection system with 3D scanning and robot technology for detecting surface dimension of the track slabs, Automation in Construction. 142 (2022) 104525. https://doi.org/10.1016/j.autcon.2022.104525.
[121] C. Yu, W. Ding, Q. Zhang, Research on a calculation method for the damage evaluation of the existing urban tunnel lining structure, Modern Tunnelling Technology. 55 (5) (2018), pp. 11–18 (in Chinese). https://doi.org/10.13807/j.cnki.mtt.2018.05.002.
[122] Y.S. Frolov, A.N. Konkov, E.S. Svintsov, Appraisal of highway tunnels construction on the active railroad tunnel operational reliability in the City of Sochi, Procedia Engineering. 189 (2017), pp. 811–817. https://doi.org/10.1016/j.proeng.2017.05.126.
[123] H. Cao, L. Peng, M. Lei, F. Chen, Q. Tang, Causes analysis, reinforcement and repair technology of segment crack and damage during shield tunnelling process: a case study, Geotechnical and Geological Engineering. 37 (2019), pp. 765–773. https://doi.org/10.1007/s10706-018-0648-y.
[124] W.N. Yiu, H.J. Burd, C.M. Martin, Finite-element modelling for the assessment of tunnel-

induced damage to a masonry building, Géotechnique. 67 (9) (2017), pp. 780–794. https://doi.org/10.1680/jgeot.sip17.P.249.
[125] W. Han, Y. Jiang, N. Li, G. Wang, H. Luan, C. Liu, Failure behavior and reinforcing design of degraded tunnel linings based on the three-dimensional numerical evaluation, Engineering Failure Analysis. 129 (2021) 105677. https://doi.org/10.1016/j.engfailanal.2021.105677.
[126] K. Kiriyama, M. Kakizaki, T. Takabayashi, N. Hirosawa, T. Takeuchi, H. Hajohta, Y. Yano, K. Imafuku, Structure and construction examples of tunnel reinforcement method using thin steel panels, Nippon Steel Technical Report. 92 (2005), pp. 45–50 https://www.nipponsteel.com/en/tech/report/nsc/pdf/n9209.pdf (Last accessed in March 12th, 2023).
[127] D. Zhang, W. Zhai, H. Huang, D. Chapman, Robust retrofitting design for rehabilitation of segmental tunnel linings: Using the example of steel plates, Tunnelling and Underground Space Technology. 83 (2019), pp. 231–242. https://doi.org/10.1016/j.tust.2018.09.016.
[128] C.T. Chang, C.W. Sun, S.W. Duann, R.N. Hwang, Response of a Taipei Rapid Transit System (TRTS) tunnel to adjacent excavation, Tunnelling and Underground Space Technology. 16 (3) (2001), pp. 151–158. https://doi.org/10.1016/s0886-7798(01)00049-9.
[129] X. Liu, Z. Jiang, Y. Yuan, H.A. Mang, Experimental investigation of the ultimate bearing capacity of deformed segmental tunnel linings strengthened by epoxy-bonded steel plates, Structure and Infrastructure Engineering. 14 (6) (2018), pp. 685–700. https://doi.org/10.1080/15732479.2017.1354892.
[130] C.T. Chang, M.J. Wang, C.T. Chang, C.W. Sun, Repair of displaced shield tunnel of the Taipei rapid transit system, Tunnelling and Underground Space Technology. 16 (3) (2001), pp. 167–173. https://doi.org/10.1016/S0886-7798(01)00050-5.
[131] X. Bi, X. Liu, X. Wang, L. Lu, Y. Zhu, Experimental study on the ultimate load-bearing capacity of deformed segmental tunnel linings strengthened by steel plates, China Civil Engineering Journal. 47 (11) (2014), pp. 128–137 (in Chinese). https://doi.org/10.15951/j.tmgcxb.2014.11.048.
[132] W. Zhai, D. Chapman, D. Zhang, H. Huang, Experimental study on the effectiveness of strengthening over-deformed segmental tunnel lining by steel plates, Tunnelling and Underground Space Technology. 104 (2020) 103530. https://doi.org/10.1016/j.tust.2020.103530.
[133] X. Liu, H. Lai, Y. Sang, Case study on the model test of staggered-jointed assembling shield tunnel structure reinforced by bonded steel plates under large deformation, IOP Conference Series: Earth and Environmental Science. 330 (2) (2019) 022080. https://doi.org/10.1088/1755-1315/330/2/022080.
[134] T. Liu, H. Huang, R. Xu, X. Yang, Research on load-bearing capacity of metro shield tunnel lining strengthened by bonded steel plates, China Journal of Highway and Transport. 30 (8) (2017), pp. 91–99 (in Chinese). https://doi.org/10.19721/j.cnki.1001-7372.2017.08.010.
[135] P. Xu, Y. Wei, Y. Yang, X. Zhou, Application of fabricated corrugated steel plate in subway tunnel supporting structure, Case Studies in Construction Materials. 17 (2022) e01323. https://doi.org/10.1016/j.cscm.2022.e01323.
[136] D. Liu, J. Zuo, J. Wang, P. Li, K. Duan, D. Zhang, S. Guo, Bending failure mechanism and strengthening of concrete-filled steel tubular support, Engineering Structures. 198 (2019)

109449. https://doi.org/10.1016/j.engstruct.2019.109449.
[137] G. Wei, Q. Wang, X. Zhou, F. Feng, X. Wang, L. Zhang, L. Liang, Experiments and numerical simulation of the reinforcement effect of channel-steel-reinforced shield tunnel segments under unloading conditions, European Journal of Environmental and Civil Engineering. (2023), pp. 1–23. https://doi.org/10.1080/19648189.2023.2177751.
[138] G. Yan, Y. Shen, B. Gao, Q. Zheng, K. Fan, H. Huang, Damage evolution of tunnel lining with steel reinforced rubber joints under normal faulting: An experimental and numerical investigation, Tunnelling and Underground Space Technology. 97 (2020) 103223. https://doi.org/10.1016/j.tust.2019.103223.
[139] Z. Li, X. Liu, H. Lai, Z. Yang, B. Wang, Detailed damage mechanism of deformed shield tunnel linings reinforced by steel plates, Engineering Failure Analysis. 143 (2023) 106850. https://doi.org/10.1016/j.engfailanal.2022.106850.
[140] Y. Sun, Y. Yu, J. Wang, Y. Ye, Q. Tan, Mechanical properties of linings of shield tunnel strengthened by steel plates considering interface effects, Chinese Journal of Geotechnical Engineering. 44 (2) (2022), pp. 343–351 (in Chinese). http://f6z.cn/0MfcL (Last accessed in March 12th, 2023)
[141] ABAQUS. Analysis user's manual version (2019). http://130.149.89.49:2080/v6.14/books/usb/default.htm (Last accessed in March 12th, 2023).
[142] M.L. Benzeggagh, M. Kenane, Measurement of mixed-mode delamination fracture toughness of unidirectional glass/epoxy composites with mixed-mode bending apparatus, Composites Science and Technology. 56 (4) (1996), pp. 439–449. https://doi.org/10.1016/0266-3538(96)00005-X.
[143] A. Yin, X. Yang, C. Zhang, G. Zeng, Z. Yang, Three-dimensional heterogeneous fracture simulation of asphalt mixture under uniaxial tension with cohesive crack model, Construction and Building Materials. 76 (2015), pp. 103–117. https://doi.org/10.1016/j.conbuildmat.2014.11.065.
[144] D. Liu, F. Wang, D. Zhang, K. Duan, Interfacial stresses of shield tunnel strengthened by a thin plate at inner surface, Tunnelling and Underground Space Technology. 91 (2019) 103021. https://doi.org/10.1016/j.tust.2019.103021.
[145] T. Ren, S. Liu, X. Liu, Experimental study of bending capacity of shield tunnel lining segment strengthened by corrugated steel, Tunnel Construction. 39 (2) (2019), pp. 317–323 (in Chinese). http://f6z.cn/PMK2B (Last accessed in March 12th, 2023).
[146] D. Liu, H. Huang, Q. Yue, Y. Xue, M. Wang, Behaviour of tunnel lining strengthened by textile-reinforced concrete, Structure and Infrastructure Engineering. 12 (8) (2016), pp. 964–976. https://doi.org/10.1080/15732479.2015.1076009.
[147] A.H. Høien, B. Nilsen, R. Olsson, Main aspects of deformation and rock support in Norwegian road tunnels, Tunnelling and Underground Space Technology. 86 (2019), pp. 262–278. https://doi.org/10.1016/j.tust.2019.01.026.
[148] X. Liu, W. Liu, Y. Sang, F. Kong, Research on failure mechanism of cracked lining reinforced with stacked inner lining, Chinese Journal of Rock Mechanics and Engineering. 34 (S2) (2015) 4244–4251 (in Chinese). https://doi.org/10.13722/j.cnki.jrme.2015.1001.
[149] W. Yu, Y. Sang, Experimental study of the deformation law of cracked tunnel lining reinforced by separated cover arch, Modern Tunnelling Technology. 51 (4) (2014) 141–149 (in Chinese). https://doi.org/10.13807/j.cnki.mtt.2014.04.021.

[150] Y. Hakoishi, H. Mashimo, T. Ishimura, S. Morimoto, A experimental study on load-carrying capacity of tunnel with the damaged lining reinforced with inner concrete reinforcement lining, in: PROCEEDINGS OF TUNNEL ENGINEERING, JSCE, Japan Society of Civil Engineers, 2003, pp. 349–354 (in Japanese). https://doi.org/10.11532/journalte1991.13.349.
[151] X. Liu, H. Lai, Y. Sang, Y. Zhang, Study on mechanics damage mechanism of arch surround reinforced structure under loose load, in: IOP Conference Series: Earth and Environmental Science, IOP Publishing, 2019, p. 022085. https://doi.org/10.1088/1755-1315/330/2/022085.
[152] X. Liu, X. Wang, B. He, Y. Sang, Model test of cracked tunnel lining reinforced with umbrella arch based on secondary loading, Journal of Sichuan University (Engineering Science Edition). 47 (3) (2015), pp. 21–28 (in Chinese). https://doi.org/10.15961/j.jsuese.2015.03.004.
[153] Y. Liu, H. Lin, X. Li, Study on the method of reinforcing with compound cover arch in existing cracked tunnels, Highway. 63 (9) (2018), pp. 289–295 (in Chinese). http://w0d.cn/qp0e (Last accessed in March 12th, 2023).
[154] F. Wang, Y. Liu, L. Wang, Detection and renovation for hazards in Chongqing Bayi Tunnel, Technology of Highway and Transport. 71 (2) (2008), pp. 112–116 (in Chinese). https://doi.org/10.3969/j.issn.1009-6477.2008.02.031.
[155] I. Laníková, P. Štěpánek, J. Venclovskỳ, Optimization of a tunnel lining reinforced with FRP, in: Key Engineering Materials, Trans Tech Publications, 2016, pp. 148–159. https://doi.org/10.4028/www.scientific.net/KEM.691.148.
[156] Z. Wu, Y. Wu, M.F.M. Fahmy, 7 - Reinforcing spalling resistance of concrete structures with bonded fiber–reinforced polymer composites, in: Z. Wu, Y. Wu, M.F.M. Fahmy (Eds.), Structures Strengthened with Bonded Composites, Woodhead Publishing, 2020, pp. 481–524. https://doi.org/10.1016/B978-0-12-821088-8.00007-2 (ISBN 9780128210895).
[157] Q. Wu, Y. Cai, Applying carbon fiber cloths to repair lining cracks in a double arched tunnel, Modern Tunnelling Technology. 43 (6) (2006), pp. 70–75 (in Chinese). https://doi.org/10.13807/j.cnki.mtt.2006.06.014.
[158] Q. Ai, Y. Yuan, X. Bi, Acquiring sectional profile of metro tunnels using charge-coupled device cameras, Structure and Infrastructure Engineering. 12 (9) (2016), pp. 1065–1075. https://doi.org/10.1080/15732479.2015.1076855.
[159] C. Yang, M. Huang, X. Liu, S. Wang, Effect of lining crack treatment using carbon fiber in deep buried tunnel, Journal of PLA University of Science and Technology (Natural Science Edition). 11 (3) (2010), pp. 322–327 (in Chinese). http://f6z.cn/sMsGI (Last accessed in March 12th, 2023).
[160] Y. Jiang, X. Wang, B. Li, Y. Higashi, K. Taniguchi, K. Ishida, Estimation of reinforcing effects of FRP-PCM method on degraded tunnel linings, Soils and Foundations. 57 (3) (2017), pp. 327–340. https:// doi.org/10.1016/j.sandf.2017.05.002.
[161] FRP Grid Method Association, Design and construction manual of the repair & reinforcement method for RC structures by FRP grid. http://www.frp-grid.com/01.html (Last accessed in February 17th, 2023).
[162] D. Liu, Q. Shang, M. Li, J. Zuo, Y. Gao, F. Xu, Cracking behaviour of tunnel lining under bias pressure strengthened using FRP Grid-PCM method, Tunnelling and Underground Space Technology. 123 (2022) 104436. https://doi.org/10.1016/j.tust.2022.104436.
[163] Y. Li, M. Wang, H. Xu, Y. Zhang, Numerical analysis of metro tunnel structure reinforced

by fiber cloth material, China Civil Engineering Journal. 47 (8) (2014), pp. 138–144 (in Chinese). https://doi.org/10.15951/j.tmgcxb.2014.08.042.
[164] Z. Liu, D. Zhang, The mechanism and effects of AFRP reinforcement for a shield tunnel in soft soil, Modern Tunnelling Technology. 51 (5) (2014), pp. 155–160 (in Chinese). https://doi.org/10.13807/j.cnki.mtt.2014.05.024.
[165] X. Liu, C. Zhang, C. Zhang, Z. Jiang, Experimental study on the longitudinal joint in shield tunnel reinforced with FRP material, Journal of Railway Science and Engineering. 13 (2) (2016), pp. 316–324 (in Chinese). https://doi.org/10.19713/j.cnki.43-1423/u.2016.02.018.
[166] D.A. Hensher, Fiber-reinforced-plastic (FRP) reinforcement for concrete structures: properties and applications, in: Elsevier, 2016. https://doi.org/10.1016/C2009-0-09136-3 (ISBN 978-0-444-89689-6).
[167] D.A. Bournas, A. Pavese, W. Tizani, Tensile capacity of FRP anchors in connecting FRP and TRM sheets to concrete, Engineering Structures. 82 (2015), pp. 72–81. https://doi.org/10.1016/j.engstruct.2014.10.031.
[168] H. Huang, L. Xiao, D. Zhang, J. Zhang, Influence of spatial variability of soil Young's modulus on tunnel convergence in soft soils, Engineering Geology. 228 (2017), pp. 357–370. https://doi.org/10.1016/j.enggeo.2017.09.011.
[169] D. Zhang, W. Zou, J. Yan, Effective control of large transverse deformation of shield tunnels using grouting in soft deposits, Chinese Journal of Geotechnical Engineering. 36 (12) (2014), pp. 2203–2212 (in Chinese). https://doi.org/10.11779/CJGE201412007.
[170] T. Zhao, T. Han, G. Wu, Y. Gao, Y. Lu, Effects of grouting in reducing excessive tunnel lining deformation: Field experiment and numerical modelling using material point method, Tunnelling and Underground Space Technology. 116 (2021) 104114. https://doi.org/10.1016/j.tust.2021.104114.
[171] H.F. Schweiger, C. Kummerer, R. Otterbein, E. Falk, Numerical modelling of settlement compensation by means of fracture grouting, Soils and Foundations. 44 (1) (2004), pp. 71–86. https://doi.org/10.3208/sandf.44.71.
[172] K. Soga, M.D. Bolton, S.K.A. Au, K. Komiya, J.P. Hamelin, A. Van Cotthem, G. Buchet, J.P. Michel, Development of compensation grouting modelling and control system, in: Proceedings of the International Symposium on Geotechnical Aspects of Underground Construction in Soft Ground, Tokyo, Japan, 1999, pp. 425–430 (in Japanese). https://cir.nii.ac.jp/crid/1573668924848886784 (Last accessed in March 12th, 2023).
[173] X. Xue, J. Zhang, G. Yao, Y. Gao, Study on mechanical property of highway tunnel lining grouting reinforcement, Journal of Highway and Transportation Research and Development. 34 (4) (2017), pp. 93–100. https://doi.org/10.3969/j.issn.1002-0268.2017.04.014.
[174] D. Liu, F. Wang, Q. Hu, H. Huang, J. Zuo, C. Tian, D. Zhang, Structural responses and treatments of shield tunnel due to leakage: A case study, Tunnelling and Underground Space Technology. 103 (2020) 103471. https://doi.org/10.1016/j.tust.2020.103471.
[175] F. Wang, M. Zhou, D. Zhang, H. Huang, D. Chapman, Random evolution of multiple cracks and associated mechanical behaviors of segmental tunnel linings using a multiscale modeling method, Tunnelling and Underground Space Technology. 90 (2019), pp. 220–230. https://doi.org/10.1016/j.tust.2019.05.008.
[176] J. Zhang, K.K. Phoon, D. Zhang, H. Huang, C. Tang, Deep learning-based evaluation of factor of safety with confidence interval for tunnel deformation in spatially variable soil,

Journal of Rock Mechanics and Geotechnical Engineering. 13 (6) (2021), pp. 1358–1367. https://doi.org/10.1016/j.jrmge.2021.09.001.
[177] D. Zhang, Z. Liu, R. Wang, D. Zhang, Influence of grouting on rehabilitation of an over-deformed operating shield tunnel lining in soft clay, Acta Geotech. 14 (4) (2019), pp. 1227–1247. https://doi.org/10.1007/s11440-018-0696-8.
[178] Z. Yang, X. Niu, K. Hou, Y. Guo, Z. Zhou, F. Chen, Y. Kang, Study on diffusion parameters of Bingham fluid based on column-hemispherical penetration grouting, Journal of Sichuan University (Engineering Science Edition). 47 (S2) (2015), pp. 47–53 (in Chinese). https://doi.org/10.15961/j.jsuese.2015.s2.008.
[179] Q. Zhang, L. Zhang, R. Liu, W. Han, M. Zhu, X. Li, D. Zheng, X. Xu, Laboratory experimental study of cement-silicate slurry diffusion law of crack grouting with dynamic water, Rock and Soil Mechanics. 36 (8) (2015), pp. 2159–2168 (in Chinese). https://doi.org/10.16285/j.rsm.2015.08.005.
[180] J. Zou, L. Li, X. Yang, Z. Wang, C. He, Method of energy analysis for compaction grouting, Rock and Soil Mechanics. 27 (3) (2006), pp. 475–478 (in Chinese). https://doi.org/10.16285/j.rsm.2006.03.029.
[181] C. Zhang, J. Fu, J. Yang, X. Ou, X. Ye, Y. Zhang, Formulation and performance of grouting materials for underwater shield tunnel construction in karst ground, Construction and Building Materials. 187 (2018), pp. 327–338. https://doi.org/10.1016/j.conbuildmat.2018.07.054.
[182] T. Wu, Y. Gao, Y. Zhou, Application of a novel grouting material for prereinforcement of shield tunnelling adjacent to existing piles in a soft soil area, Tunnelling and Underground Space Technology. 128 (2022) 104646. https://doi.org/10.1016/j.tust.2022.104646.
[183] S. Li, P. Wang, C. Yuan, J. Li, P. Ma, B. Zhi, H. Zhou, Y. Tian, Adaptability of polyurethane/water glass grouting reinforcement to subsea tunnels, Construction and Building Materials. 311 (2021) 125354. https://doi.org/10.1016/j.conbuildmat.2021.125354.
[184] J. Liu, O. Hamza, K.S. Davies-Vollum, J. Liu, Repairing a shield tunnel damaged by secondary grouting, Tunnelling and Underground Space Technology. 80 (2018), pp. 313–321. https://doi.org/10.1016/j.tust.2018.07.016.
[185] Z. Saleheen, R.R. Krishnamoorthy, A. Nadjai, A review on behavior, material properties and finite element simulation of concrete tunnel linings under fire, Tunnelling and Underground Space Technology. 126 (2022) 104534. https://doi.org/10.1016/j.tust.2022.104534.
[186] S. Sony, K. Dunphy, A. Sadhu, M. Capretz, A systematic review of convolutional neural network-based structural condition assessment techniques, Engineering Structures. 226 (2021) 111347. https://doi.org/10.1016/j.engstruct.2020.111347.
[187] D. Ai, G. Jiang, S.K. Lam, P. He, C. Li, Computer vision framework for crack detection of civil infrastructure—A review, Engineering Applications of Artificial Intelligence. 117 (2023) 105478. https://doi.org/10.1016/j.engappai.2022.105478.
[188] T. Hao, C.D.F. Rogers, N. Metje, D.N. Chapman, J.M. Muggleton, K.Y. Foo, P. Wang, S.R. Pennock, P.R. Atkins, S.G. Swingler, J. Parker, S.B. Costello, M.P.N. Burrow, J.H. Anspach, R.J. Armitage, A.G. Cohn, K. Goddard, P.L. Lewin, G. Orlando, M.A. Redfern, A.C.D. Royal, A.J. Saul, Condition assessment of the buried utility service infrastructure, Tunnelling and Underground Space Technology. 28 (2012), pp. 331–344. https://doi.org/10.1016/j.tust.2011.10.011.

[189] S. Sajid, L. Chouinard, Impulse response test for condition assessment of concrete: A review, Construction and Building Materials. 211 (2019), pp. 317–328. https://doi.org/10.1016/j.conbuildmat.2019.03.174.

1 ***Appendix 1 Literature reviews for defect detection methods in infrastructures***

2

References	Year	Subject of investigation	Method	Major findings and remarks
Feng and Feng [16]	2018	Civil infrastructure defects	Computer vision	The paper presents general principles of the vision sensor systems, introduces the performance evaluation experiments of vision sensors and the application of displacement measurement data for SHM. Vision sensors still need improvements in accuracy, resolution and robustness.
Koch et al. [19]	2015	Civil infrastructure defects	Computer vision	The paper reviews computer vision-based methods for defect detection and condition assessment. In precast concrete tunnels, data collection and location detection of defects are fully automated. Poor lighting conditions, irregularly patterned background and contrast as well as limited data quality and quantity impose the most significant problems.
Attard et al. [10]	2018	Tunnel defects	Photogrammetric techniques, image processing and computer vision	This review summarizes the state of the art in vision-based automation technologies used in different tunnel inspection procedures and presents a comprehensive review focusing on image-based tunnel inspection.
Hsieh and Tsai [18]	2020	Structure cracks	Machine Learning	The author organizes and provides up-to-date information on the research of ML-based crack detection algorithms, and reviews 68 ML-based crack detection papers in detail to identify the current development trend. A performance evaluation system should be established to qualitatively and objectively evaluate crack detection algorithms.
McCann and Forde [21]	2001	Concrete and masonry structure defects	NDT methods	As a highly representative review, it reviews a wide range of NDT techniques applied to bridges and buildings. The author describes five major factors that influence the success of a survey: depth of penetration, vertical and lateral resolution, contrast in physical properties, signal-to-noise ratio and existing information about the structure.
Lai et al. [22]	2018	Civil engineering defects	GPR	This paper reviews the latest development of the GPR's primary infrastructure applications. Different types of tunnel linings can be surveyed by GPR, except shotcrete containing steel fibers. The air-coupled GPR can indicate areas of high moisture or low density (high air voids), while ground-

				coupled GPR can possibly detect defects at different cover depths within or just behind the tunnel linings.
Schabowicz [23]	2015	Concrete structure defects	Acoustic techniques	This paper introduces modern acoustic techniques to detect unilaterally accessible concrete structures. A combination of the impulse response technique and ultrasonic tomography is recommended for identifying and locating zones of concrete macroheterogeneities. A combination of nondestructive techniques using ultrasonic tomography and impact-echo is then recommended to determine the depth of cracks. These methods have been validated in situ.
Montero et al. [24]	2015	Tunnel defects	Robotic inspection system	The paper presents the key aspects of tunnel inspection and a survey of the developed robotic tunnel inspection systems to date. It is still very difficult for robots to perform fully automated tunnel inspections. In addition, factors such as communication, data transmission, data quality, and objectivity also need to be considered.

1
2
3
4

Appendix 2 Literature reviews for structural condition assessment methods

References	Year	Subjects	Major findings and remarks
Saleheen et al. [185]	2022	Evaluation	Numerical simulation methods for damage assessment of tunnel linings under fire were reviewed. The behaviour and material properties of concrete at elevated temperatures are shown in this review, which is useful for researchers modelling tunnel linings under fire.
Sony et al. [186]	2021	Detection and evaluation	The article reviews the implementation of convolutional neural networks (CNNs) in structural health monitoring. The authors have provided a detailed analysis and discussion of the current state and problems of research on structural condition assessment based on CNNs. The challenges and solutions to structural condition assessment need to be studied in depth.
Ai et al. [187]	2023	Detection and evaluation	A review of vision-based crack detection and assessment methods. Although the main subject of this paper is cracks, it is still helpful in assessing the overall condition of the tunnel.

Alsharqawi et al. [27]	2022	Detection and evaluation	This paper describes the current state of knowledge on the use of ground penetrating radar (GPR) to assess concrete structures. Based on the inadequacy of current studies, it is recommended that research directions should be focused on in the future. Further research is expected on data processing and the selection of assessment indicators.
Hao et al. [188]	2012	Evaluation	This paper provides an overview of various condition assessment techniques for buried utility services. Challenges remain in resolving the weaknesses of different assessment techniques
Sajid and Chouinard [189]	2019	Detection and evaluation	The first review of the researches related to the impulse response test. The basic principles and issues faced in impulse response test-based evaluation techniques are summarized. The authors have identified current knowledge gaps and provided recommendations to overcome the issues.

1
2
3
4

Appendix 3 Literature reviews for tunnel lining retrofitting

References	Year	Subjects	Major findings and remarks
Asakura and Kojima [31]	2003	Tunnel detection Retrofitting	The paper summarizes the inspection and retrofitting methods actually used for railway tunnels in Japan. Moreover, three cases are shown: one of them is the Tukayama tunnel concerning countermeasures against plastic earth pressure and the others are the Fukuoka tunnel and the Rebunhama tunnel concerning an accident caused by spalling of tunnel lining.
Richards [32]	1998	Tunnel detection Retrofitting	The paper briefly summarizes tunnel detection and retrofitting methods but lacks a detailed description of the development and application of retrofitting methods, including their advantages and disadvantages. The results demonstrate that the design of tunnel structures should take account of new inspection technologies, thereby reducing costs of inspections and disruptions as well as providing for more cost-effective preventative maintenance and repair.
Ye et al. [33]	2021	Tunnel defects Retrofitting	This paper describes the application of tunnel retrofitting technology in China and examines five characteristics of tunnel defects. In turn, feasible defect prevention and treatment procedures were proposed.

Sousa et al. [34]	2009	Tunnel retrofitting	This paper presents a technique for modeling decisions under uncertainty, BN, and their “extension” to Influence Diagrams. An example applied to the maintenance of tunnels was presented, with the intent of illustrating the advantages and potential of this technique when applied to real problems.
Rock et al. [35]	2006	Tunnel retrofitting Evaluation	Methods for maintaining, renovating, and improving road tunnels are outlined, including assessments of potential threats and vulnerabilities. The results demonstrate that tunnel cracking is the most damaging condition to the structural performance of a tunnel
Liu and Zhu [36]	2005	Tunnel defects Retrofitting	An in-depth analysis of the causes of the defects is conducted for the double-arch tunnel. Appropriate preventive and corrective actions are then proposed to address the issue.
Luo and Chen [37]	2019	Tunnel defects Retrofitting	An evaluation of the current state and advancement of tunnel damage was conducted, and a thorough analysis of the key measures for preventing and managing frost damage was performed. The results demonstrate that the current theoretical model for tunnel assessment is not very accurate and needs further development.
Feng et al. [38]	2019	Tunnel defects Retrofitting	The paper presents a case study of the sidewall cracking problem in an existing tunnel and proposes a solution to the problem verified by numerical analysis. The results demonstrate that groundwater has weakened the physical and mechanical properties of the surrounding rock and is the main cause of tunnel wall cracking.
Ye et al. [39]	2020	Tunnel defects Retrofitting Evaluation	The paper investigates the occurrence of tunnel lining defects in the G312 Liupanshan Highway Tunnel in Guyuan City and analyzes the damage characteristics, occurrence mechanisms, and reinforcement methods by combining external and internal causes.
Zhang et al. [40]	2020	Tunnel defects Retrofitting	This paper presents the retrofitting methods and the design principles for repairing tunnels damaged by earthquakes, taking the Tawarayama Tunnel as a case study. The results demonstrate that spalling/collapse of liners due to ground vibrations and groundwater leaks have a significant impact on the design of retrofitting.

1